UNIVERSITY OF CALIFORNIA, SAN DIEGO
SCRIPPS INSTITUTION OF OCEANOGRAPHY
VISIBILITY LABORATORY
SAN DIEGO, CALIFORNIA 92152

PROGRESS IN IMAGE PROCESSING TECHNIQUES AND EQUIPMENT

Benjamin L. McGlamery, Madison L. Myers,
Richard L. Ensminger, Robert F. Howarth

FINAL REPORT
Advanced Research Projects Agency
Contract No. F08606-68-C-0017, MOD P003
Effective Date: 1 September 1968
Expiration Date: 31 August 1969
Principal Investigator: James L. Harris, Sr.
Phone: 714-453-2000, X306

SIO Ref. 69-28
November 1969

Advanced Research Projects Agency
Washington, D. C. 20301

Approved:

S. Q. Duntley

Seibert Q. Duntley, Director
Visibility Laboratory

Approved for Distribution:

John D. Isaacs

John D. Isaacs, Acting Director
Scripps Institution of Oceanography

TABLE OF CONTENTS

Page

LIST OF FIGURES

LIST OF TABLES

FOREWORD

The Visibility Laboratory has been engaged in an extended research program on image processing. This research has been directed toward the development of techniques by which man can be aided in the extraction of information from degraded images. Emphasis has been on images degraded by atmospheric turbulence although other forms of degradation which could be encountered in an optical system, such as image motion and defocus, have been considered. The research has been concerned with several broad areas: theoretical studies, computer implementation of processing techniques, simulation studies, processing on real images, sensor studies, and development of scanning and display equipment.

This report reflects the current emphasis on processing techniques and describes the present physical facilities by which image processing is implemented at the Visibility Laboratory. The report consists of five sections. Section one compares the effectiveness of several processing techniques applied to degraded images containing various amounts of noise. Section two reports the results of studies for the determination of the noise characteristics pertinent to image processing for several sensors. Section three describes the computer facility and image processing programs at the Visibility Laboratory. Section four describes currently operational scanning and display equipment. Section five provides a brief summary.

Some of the material in this report has been transmitted previously in the form of informal memos. It is included in this report for broader distribution.

ABSTRACT

This report describes the current emphasis of image processing research at the Visibility Laboratory. The following aspects of the work are described: image processing studies, sensor studies, the image processing computer system and image processing equipment. The image processing studies compare the performance of different methods of image restoration as a function of noise level in the degraded image. The sensor studies compare the noise characteristics for several different sensors used for recording images. The capabilities of the computer system used for image processing and the program philosophy are described. The characteristics of the image scanning and display systems used as input and output devices for the image processing facility are reported.

1.0 IMAGE PROCESSING STUDIES

1.1 Introduction

The feasibility of improving turbulence degraded images by post-recording processing has been demonstrated by laboratory experiments.[1,2,3] In these experiments factors such as sensor noise, sensor non-linearities, non-isoplanatism of the point spread function, and incomplete knowledge of the point spread function were purposely minimized. The success of these experiments has demonstrated the basic feasibility of restoration under ideal conditions. With this important step accomplished, we now need to learn the limitations imposed on the quality of the restored image by the factors which will be encountered in practice. One of the most important of these factors is the presence of noise in the recorded degraded image. This memorandum will describe an empirical study made to determine the effects of noise in the degraded image on the quality of the restored image.

The approach taken was to make a computer simulation of the entire process from image degradation to restoration. A block diagram of the experiment is shown in Fig. 1. An image was degraded with a point spread function, noise was added, and the resulting image was processed by

---

1 James L. Harris, Sr., J. Opt. Soc. Amer. 56, 569 (1966)

2 B. L. McGlamery, Scripps Institution of Oceanography, Report 66-10, 1966.

3 B. L. McGlamery, J. Opt. Soc. Amer. 57, 293 (1967).

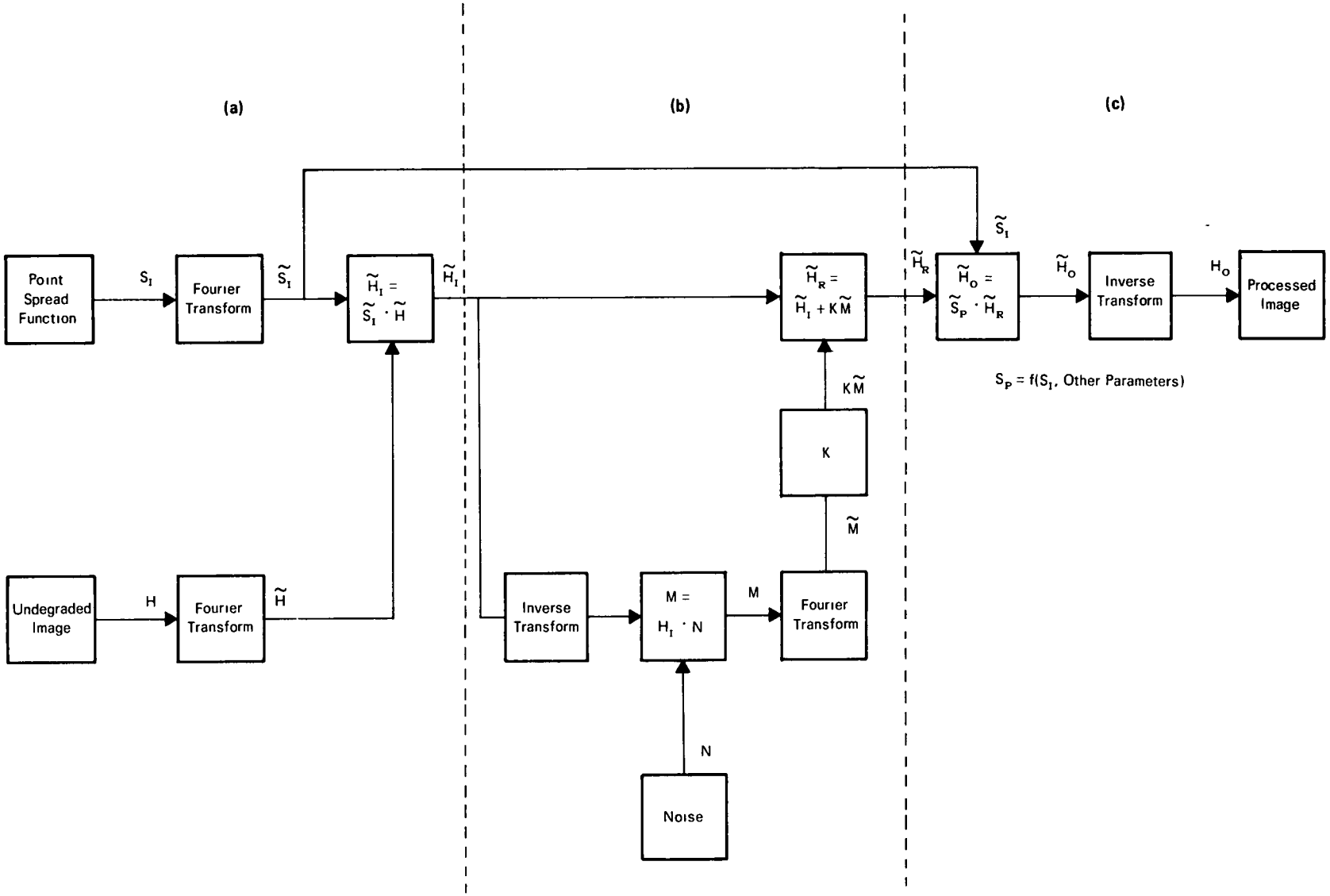

Fig. 1. Block diagram of the experiment. (a) Generation of the degraded image. (b) Generation of the multiplicative noise. (c) The restoration process.

several different techniques. All of the techniques utilized full knowledge of the point spread function. Processing techniques which might be used when the point spread function is not known are discussed in Section 1.7. The initial image was chosen to represent detail of various sizes on a target at a typical distance for some applications. The point spread function used to degrade this object was one obtained from a large aperture telescope. The noise added to the degraded image was multiplicative in nature to simulate the multiplicative nature of film noise. Thus an attempt was made to make the experiment correspond partly to conditions which might be encountered in practice. The simulation was not perfect since the exact multiplicative noise properties of film were not simulated, and effects due to finite grain size and clumping were ignored. Also the modulation transfer function of the film was not applied. However, the results obtained should be at least indicative of the effect of similar noise levels in film. As the ability to simulate film noise is improved, more accurate experiments will be made.

1.2 The Target and Point Spread Function

The undegraded image and its spectrum are shown in Fig. 2. This image was chosen to represent detail of various sizes and contrasts which might be encountered on a natural object. Object sizes are 1, 2, 4, and 8 picture elements. For a specific application these sizes are easily converted to object space size by multiplication by the appropriate scaling constant. The targets are shown at contrasts of -1, -.75, -.5, and -.25 representing reflectances of 0, .25, .5, and .75 referenced to a background reflectance of 1.0.

The point spread function used to degrade the image is shown in Fig. 2b, along with its spectrum. This image is a short exposure (about 1/100 second) photograph of a star image recorded by a 48 inch diameter telescope. The spread of this image was primarily determined by atmospheric turbulence although it does include the effects of diffraction at the entrance pupil of the telescope. The angular scale of the image is .17 arc seconds per step. If a range to the object is assumed the object space resolution element size can be determined by multiplying the angular step size in radians by the range. Scaling changes can also be made on the point spread function to simulate turbulence levels of greater or lesser magnitude. This can be done only as long as the assumed size of the point spread function remains significantly larger than the point spread function due to diffraction at the entrance pupil alone.

The degraded image and its spectrum are shown in Fig. 2c. The degraded image was obtained by effectively convolving the point spread function with the undegraded image. This was done by Fourier transforming the point spread function and the undegraded image, multiplying these Fourier transforms, and computing the inverse transform of the product.

1.3 Outline of Experiment

1.3.1 Definitions

For convenience the following definitions are used.

- r - The (x,y) coordinate in the spatial domain.
- f - The (f_x, f_y) coordinate in the frequency domain.
- $H(r)$ - The ideal or undegraded image.
- $S_I(r)$ - The input point spread function.

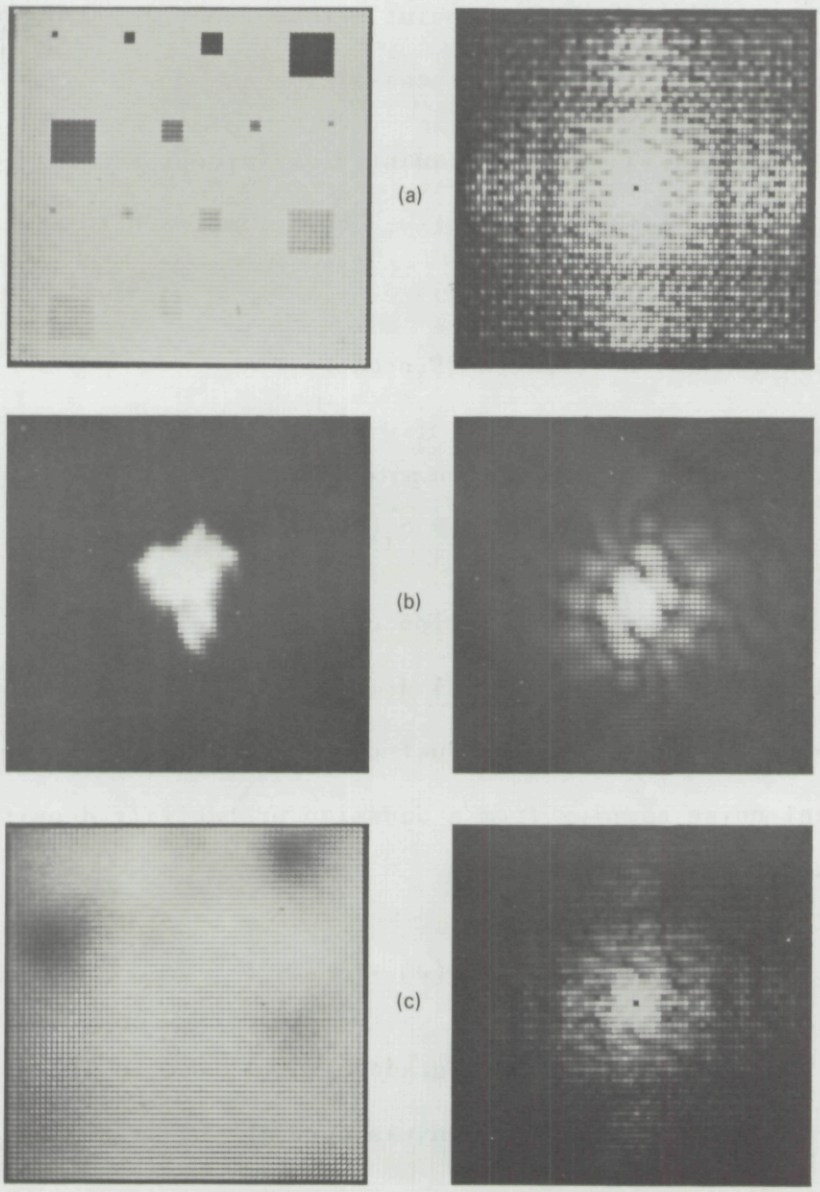

Fig. 2. (a) The undegraded image and its spectrum. (b) The point spread function and its spectrum. (c) The degraded image and its spectrum. The degraded image is shown at a gamma of 4. The spectrum pictures are shown at a gamma of .5.

$H_I(r)$ - The input or degraded image (noiseless).

$N(r)$ - An array of white Gaussian noise with unity standard deviation.

$M(r)$ - An array of multiplicative noise.

$H_R(r)$ - The recorded image (with noise).

$S_P(r)$ - The processing point spread function.

$H_0(r)$ - The output or processed image.

A tilde ($\sim$) over any of the above quantities (except r and f) indicates the Fourier transform of that quantity. For example $\widetilde{H}(f)$ is the Fourier transform of $H(r)$.

1.3.2 Degradation and Restoration Procedure

The experiment outlined in Fig. 1 will now be explained in more detail. The degraded image transform was computed from

$$\widetilde{H}_I(f) = \widetilde{S}_I(f) \cdot \widetilde{H}(f) , \qquad (1)$$

which is equivalent to the convolution of the undegraded image and the point spread function in the spatial domain. The noise component of the image was found by forming the product of the degraded image and an array of independent noise samples from a Gaussian probability density function of unity variance.

$$M(r) = H_I(r) \cdot N(r) . \qquad (2)$$

Addition of this quantity to the degraded image produced the recorded image. For convenience the addition was done in the frequency domain.

$$\widetilde{H}_R(f) = \widetilde{H}_I(f) + K\widetilde{M}(f) \qquad (3)$$

The parameter K was used to set the noise level. For example, for K= .1 the noise added to an element in the spatial domain had, over an ensemble average, a standard deviation equal to .1 of the value of that element. The degraded spectrum was then multiplied by $\widetilde{S}_P$, the restoration filter, to produce the output, or restored, image spectrum.

$$\begin{aligned}\widetilde{H}_0(f) &= \widetilde{S}_P(f) \cdot \widetilde{H}_R(f) \\ &= \widetilde{S}_P(f)\left[\widetilde{H}_I(f) + K\widetilde{M}(f)\right]. \end{aligned} \tag{4}$$

Several different forms of $\widetilde{S}_P(f)$ were used in order to compare the effectiveness of various processing methods. These are described below. Finally the inverse transform was taken of $\widetilde{H}_0(f)$ to obtain $H_0(r)$, the restored image.

1.4 Processing Methods

The various methods of processing used were the direct inverse filter, the low-pass inverse filter, the least squares filter, and the modified least squares filter.

1.4.1 Direct Inverse Filter

The direct inverse filter is the reciprocal of the optical transfer function.

$$\widetilde{S}_P(f) = \frac{1}{\widetilde{S}_I(f)} . \tag{5}$$

Substitution of this quantity into Eq. (4), the expression for the output image transform, and expressing $\widetilde{H}_I(f)$ in terms of Eq. (1) gives

$$\widetilde{H}_0(f) = \frac{1}{\widetilde{S}_I(f)}\left[\widetilde{S}_I(f)\,\widetilde{H}(f) + K\widetilde{M}(f)\right]$$

$$= \widetilde{H}(f) + \frac{K\widetilde{M}(f)}{\widetilde{S}_I(f)} \quad . \tag{6}$$

In Eq. (6) $\widetilde{H}(f)$ is the desired result and the second term of the equation represents the error due to noise. This restoration method gives a good restoration only when $\widetilde{H}(f) \gg K\widetilde{M}(f)/\widetilde{S}_I(f)$. If this condition is not satisfied then even small regions of the frequency domain where $KM(f)/\widetilde{S}_I(f) \gg \widetilde{H}(f)$ can dominate the restored image in the spatial domain.

1.4.2 Low-Pass Inverse Filter

Usually there is a portion of the spectrum at the lower spatial frequencies in which the condition $\widetilde{H}(f) \gg K\widetilde{M}(f)/\widetilde{S}_I(f)$ is satisfied. If this region is used in the restoration but the higher frequencies are omitted an improved restoration may be obtained. For this case the processing filter, $\widetilde{S}_p(f)$, becomes

$$\widetilde{S}_p(f) = \begin{cases} \dfrac{1}{\widetilde{S}_I(f)} \;, & f \leq f_{co} \\ \\ 0 \;, & f \gg f_{co} \end{cases} \tag{7}$$

where f_{co} is the maximum frequency at which the condition $\widetilde{H}(f) \gg K\widetilde{M}(f)/\widetilde{S}_I(f)$ is approximately satisfied. A disadvantage of this method is that there may be regions of the spectrum beyond f_{co} in which the low noise condition is satisfied but which are surrounded by regions in which the condition is not satisfied.

1.4.3 Least Squares Filter

The least squares filter, adapted to image processing by Helstrom[4] and Slepian[5], is based on the criteria of adjusting the spectrum of the restored image such that the mean squared error between the restored image and the undegraded image is a minimum over an ensemble average. For this filter $\widetilde{S}_P(f)$ takes the form of

$$\widetilde{S}_P(f) = \frac{S_I^*(f)|\widetilde{H}(f)|^2}{|\widetilde{S}_I(f)|^2|\widetilde{H}(f)|^2 + \overline{|K\widetilde{M}(f)|^2}} \tag{8}$$

$\overline{|K\widetilde{M}(f)|^2}$ is the spectral density of the noise taken over an ensemble of images. For convenience let $\sigma^2(f) = \overline{|K\widetilde{M}(f)|^2}$. Rearrangement of Eq.(8) produces the form

$$\widetilde{S}_P(f) = \frac{1}{\widetilde{S}_I(f)\left[1 + \dfrac{\sigma^2(f)}{|\widetilde{S}_I(f)|^2|\widetilde{H}(f)|^2}\right]}. \tag{9}$$

According to Eq. (9) the least squares filter can be viewed as a direct inverse filter of $1/\widetilde{S}_I(f)$ followed by a post-inverse filter of value

$$G(f) = \frac{1}{\left[1 + \dfrac{\sigma^2(f)}{|\widetilde{S}_I(f)|^2|\widetilde{H}(f)|^2}\right]}. \tag{10}$$

[4]Carl W. Helstrom, J. Opt. Soc. Amer. 57, 297, (1967).

[5]David Slepian, J. Opt. Soc. Amer. 57, 918, (1967).

The least squares filter requires the knowledge of the power spectrum of the undegraded image, $|\widetilde{H}(f)|^2$. Normally this quantity would not be available since the purpose of the processing is to find $\widetilde{H}(f)$. Ignoring this problem for the moment, interesting insight into the action of the least squares filter can be gained by the substitution of

$$|\widetilde{H}_I(f)|^2 = |\widetilde{S}_I(f)|^2 |H(f)|^2 \tag{11}$$

into Eq. (10). $\widetilde{S}_P(f)$ then becomes

$$\widetilde{S}_P(f) = \frac{1}{\widetilde{S}_I(f)} \left[\frac{1}{1 + \dfrac{\sigma^2(f)}{|\widetilde{H}_I(f)|^2}} \right]. \tag{12}$$

This form has a simple interpretation. At those frequencies for which $|H_I(f)|^2 \gg \sigma^2(f)$ then $\widetilde{S}_P(f) \approx 1/\widetilde{S}_I(f)$. Also, according to Eq. (3), $\widetilde{H}_R(f) \approx \widetilde{H}_I(f)$, i.e., the recorded image spectrum is a faithful representation of the noiseless degraded image. The restored spectrum is

$$\widetilde{H}_0(f) = \widetilde{H}_R(f)\, \widetilde{S}_P(f) \approx \frac{\widetilde{H}_I(f)}{S_I(f)} = \widetilde{H}(f), \tag{13}$$

so that a near-perfect restoration is obtained for those frequencies. If, however, the recorded image spectrum is dominated by noise so that $\sigma^2(f) \gg |\widetilde{H}_I(f)|^2$ then

$$\widetilde{S}_P(f) = \frac{1}{\widetilde{S}_I(f)} \cdot G(f) \tag{14}$$

where $G(f)$, given by Eq. (10), is a small factor which attenuates $\widetilde{S}_P(f)$.

Thus those frequencies at which noise dominates the recorded image spectrum are selectively suppressed in the restored image. This attenuation is done in a manner which minimizes the mean squared error.

1.4.4 Modified Least Squares Filter

One method of overcoming the need for $|\widetilde{H}(f)|^2$ in the least squares filter is to approximate it by an analytic function. This function would be chosen on the basis of knowledge about the gross properties of the image. It would have about the same rate of fall off with f as $|\widetilde{H}(f)|^2$ but would not contain the detailed variations of $|\widetilde{H}(f)|^2$. Hence the filter would no longer be sensitive to the valleys and nulls of the ideal image spectrum which produce values of $|\widetilde{H}_I(f)|^2 \lessapprox \sigma^2(f)$. It would still respond to valleys and nulls of $\widetilde{S}_I(f)$.

1.5 Experimental Results

The four processing methods described above were applied to the noisy degraded images. The value of K was set at .001, .003, .01, .03, and .10, corresponding to multiplicative noise factors ranging from .1% to 10%. Only the results for .1%, 1%, and 10% are shown here since the changes between the smaller steps were not dramatic. The noisy degraded images are shown in Fig. 3. For the restored images the contrast of the data used to generate each photograph was adjusted to make the variations in the background of the image easily visible. The restored spectrum for each image is also shown. In these images the display contrast was set so that most of the spectrum could be seen. Also the center picture of the spectrum photographs, representing the d.c. level of the picture, was suppressed so that it would not expend the dynamic range of the display

at the expense of the rest of the spectrum.

The results of using the direct inverse filter are shown in Fig. 4 where both the restored spectra and restored images are shown. At the .1% noise level the character of the spectrum of the undegraded image can be seen at the lower frequencies. At the high frequencies the effects of the noise are obvious and several very high noise peaks can be seen. The effects of the high spectrum values on the restored image are disastrous, even at the .1% level. At the higher noise levels the noise free regions of the spectra become smaller, and the restored images are very bad.

For the low-pass inverse filter f_{co} was adjusted at each noise level to give the subjectively-best restored images. The results are shown in Fig. 5. Use of the filter improved the restorations considerably over the direct inverse filter.

Since $|\widetilde{H}(f)|^2$ was available in this experiment, the least squares filter could be applied. The results are shown in Fig. 6. The selective filtering process of the least squares filter is dramatically evident in the restored spectra.

For the modified least squares filter an analytic function which approximated the rate of fall off of $|\widetilde{H}(f)|^2$ was substituted for $|\widetilde{H}(f)|^2$ in the least squares filter. The results are shown in Fig. 7. Here it can be seen that to a large extent the selective filtering process of the least squares filter has been lost. This is because the analytic function used in place of $|\widetilde{H}(f)|^2$ did not contain the many local variations of $|\widetilde{H}(f)|^2$. However, the restorations are still fair. They could possibly be improved by a different choice of the analytic function used for $|\widetilde{H}(f)|^2$.

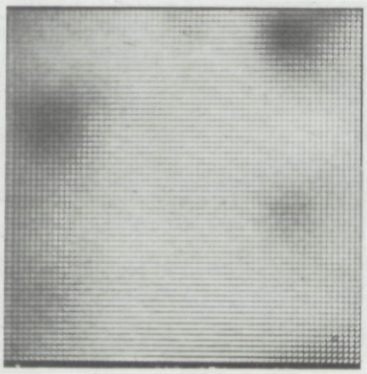

(a)

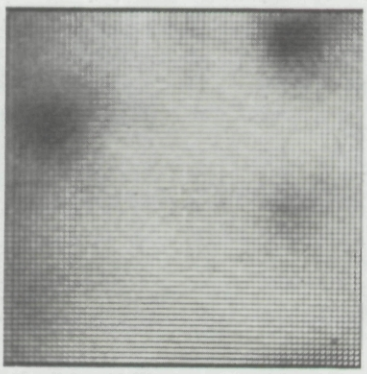

(b)

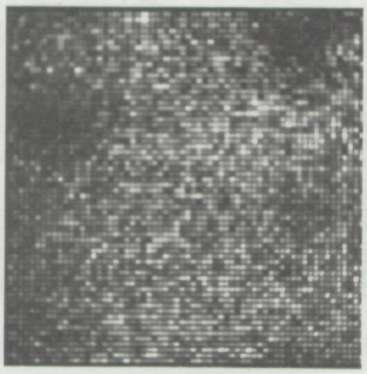

(c)

Fig. 3. The degraded image with multiplicative noise added, display gamma = 4.0. (a) .1% noise level; (b) 1%; (c) 10%.

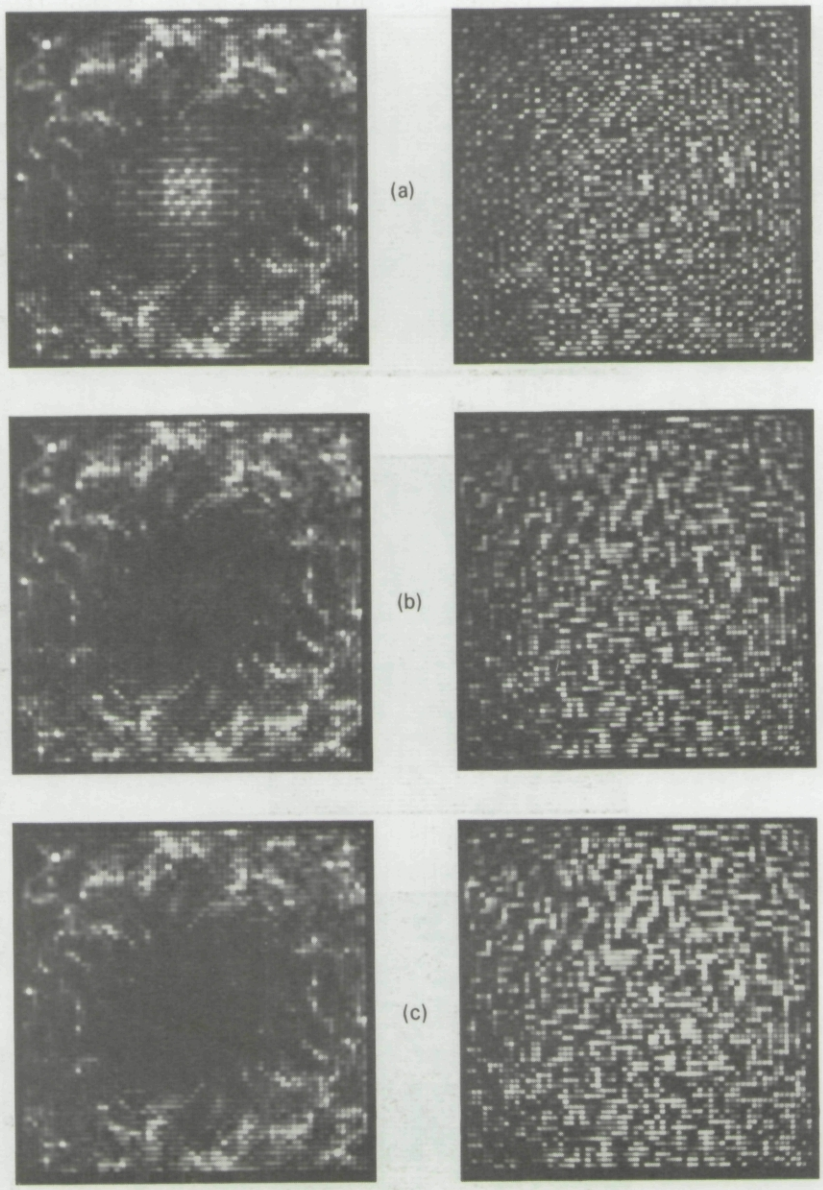

Fig. 4. Restoration by the direct inverse filter. Left: restored spectra, display gamma = .5. Right: restored images, display gamma = 1.0. (a) .1% noise level; (b) 1%; (c) 10%.

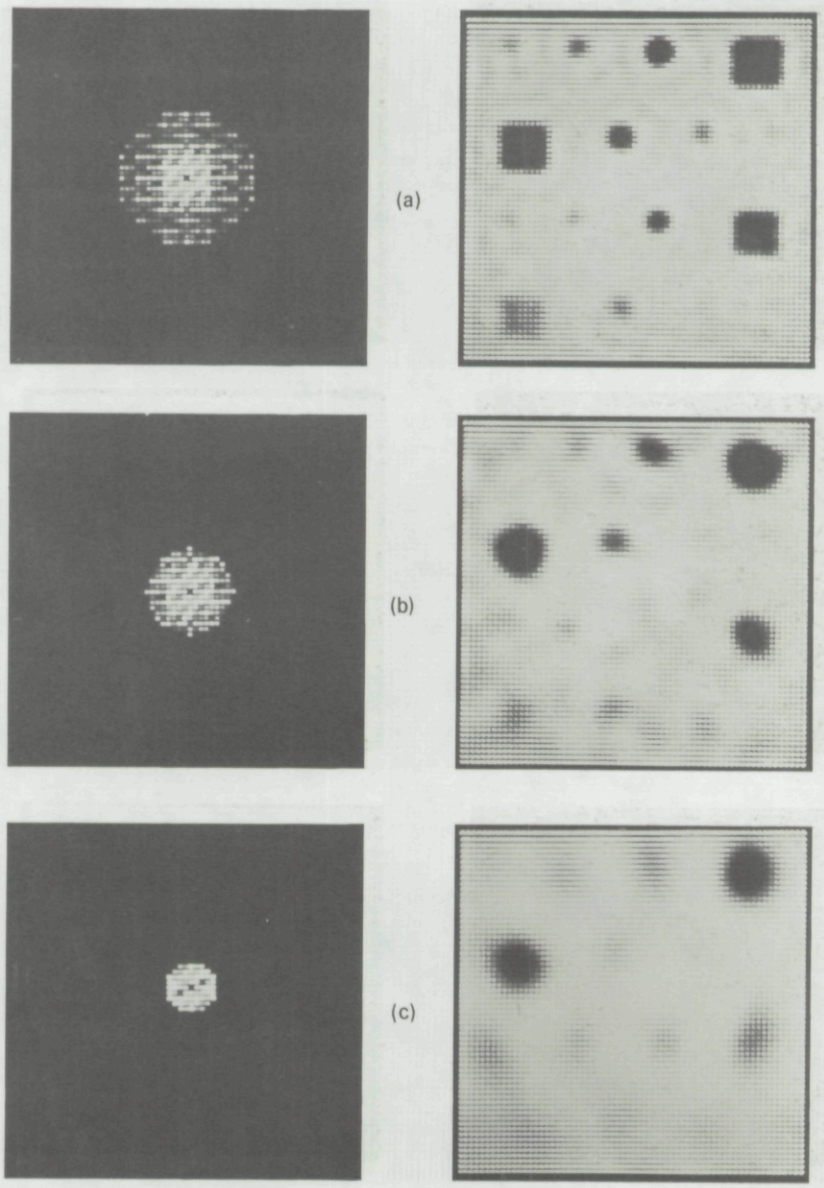

Fig. 5. Restoration by the low-pass inverse filter. Left: restored spectra, display gamma = 1.0. Right: restored images. (a) .1% noise level, display gamma = 2.0; (b) 1%; gamma = 3.0; (c) 10%, gamma = 2.0.

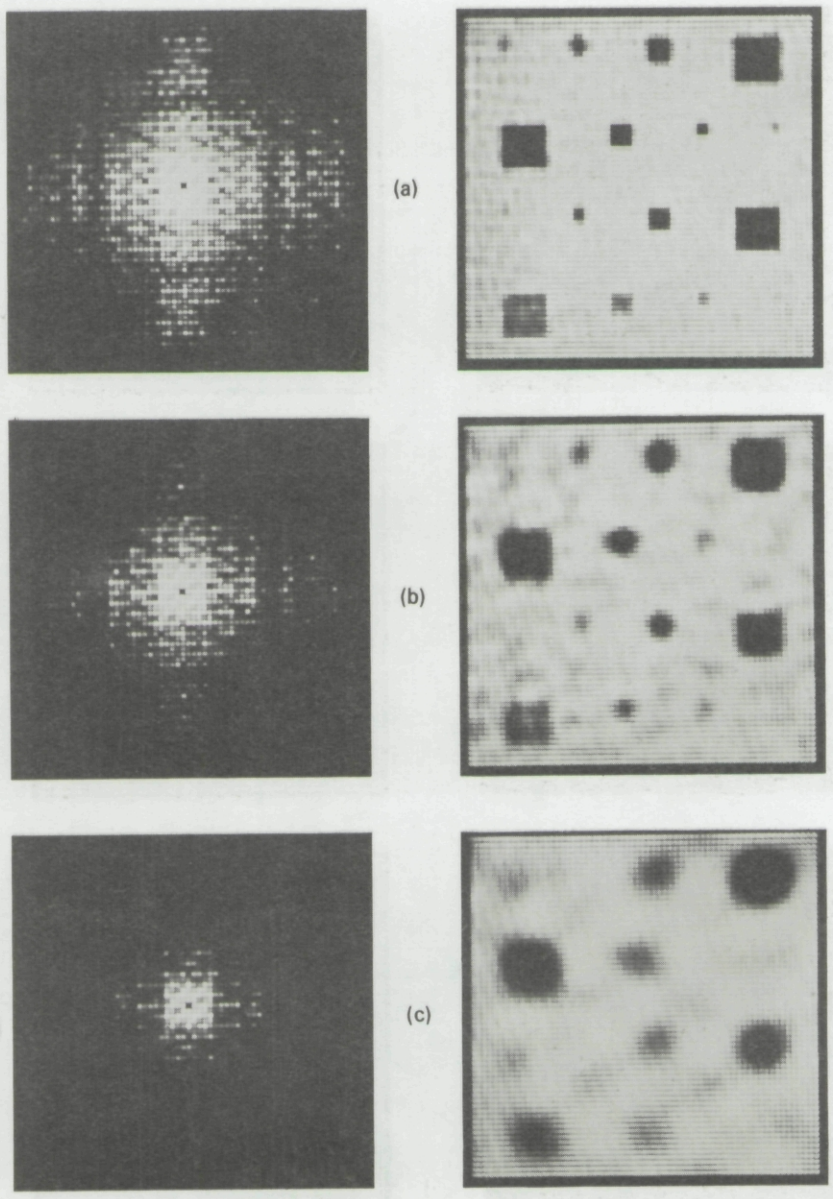

Fig. 6. Restoration by the least squares filter. Left: restored spectra, display gamma = .5. Right: restored images, display gamma = 4.0. (a) .1% noise level; (b) 1%; (c) 10%.

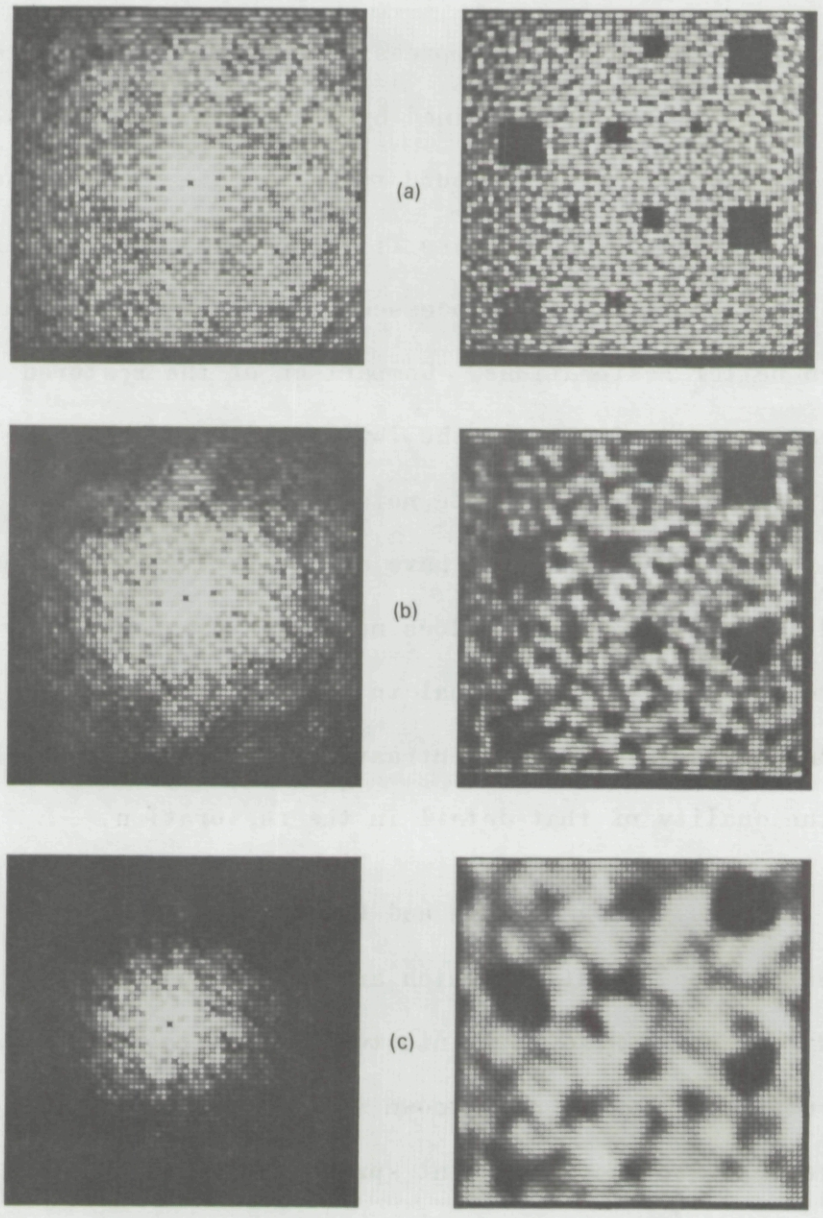

Fig. 7. Restoration by the modified least squares filter. Left: restored spectra, display gamma = .5. Right: restored images, display gamma = 4. (a) .1% noise level; (b) 1%; (c) 10%.

1.6 Discussion of Results

A quantitative comparison of the results of the four methods of processing would require the establishment of some criteria for image quality along with repeated processings using different random noise patterns. However, a subjective impression of the relative effectiveness of the four methods is easily obtained by inspection of the results.

The direct inverse filter is found to be practically useless, even at the .1% noise level. The low-pass filter results in images that are significantly better than the unprocessed image. The least squares filter produces even better restorations. Comparison of the restored spectra using the least squares filter to the low-pass filter shows the ability of the least square filter to attenuate noisy frequencies while at the same time pass higher frequencies which have an adequate signal to noise ratio. The modified least squares filter does not have this capability since it does not have knowledge of the signal to noise ratio at all parts of the spectrum. In all cases size and contrast of the object detail have a strong bearing on the quality of that detail in the restoration.

1.7 Present Work and Future Plans

Other restoration techniques which are presently being studied will be briefly discussed. These fall into two broad categories: restoration when the point spread function is known so that the limiting factor is noise, and restoration when the point spread function is not known.

In the first category part of the studies being made are an extension of the noise filtering work presented in this report. Using the least squares filtering concept as a standard, ways are being sought by which

those regions of the spectrum at which the signal to noise ratio is low can be selectively attenuated without the need for knowledge of the power spectrum of the undegraded image. A second type of processing designed to process images in which noise is a significant factor employs new concepts completely separate from those of Fourier processing. This is an iterative technique applied in the spatial domain. Initial results have in some cases produced restored images equivalent in visual information content as obtained with Fourier techniques but without the spurious ringing that is sometimes encountered with Fourier techniques. A paper describing this work is being submitted to the Journal of the Optical Society of America by W. Hadley Richardson; therefore, it will not be described in detail in this report.

The second category, i.e., processing in the absence of knowledge of the point spread function is very important, especially for the case of atmospherically degraded images. In this case restoration using only a single degraded image must rely upon some a priori knowledge of the undegraded object and the point spread function. Two pieces of a priori knowledge which are usually available are that the object and point spread function are spatially bounded and that they have non-negative irradiance maps. A restoration technique has been developed which begins with the degraded image and an assumed undegraded image and then repeatedly computes point spread functions and restored images, forcing at each step the spatially bounded and non-negative conditions. Initial results are very encouraging, with the processing producing a restored image which, while not perfect, is a definite improvement over the degraded image. A considerable amount of effort will be spent in the future on this and similar techniques. Another method of

image restoration of turbulence degraded images when the point spread function is not known involves the use of multiple degraded images. This area is receiving a limited amount of work.

Finally, the most fundamental approach to image processing involves statistical decision theory. This has been treated by Harris.[6] Utilization of this theory should lead to the ability to successfully process images at lower signal to noise ratios than by the filtering techniques described in this report. The problems to be encountered in this type of processing and the potential gain will be the subject of future studies.

2.0 SENSOR STUDIES

2.1 Introduction

Sensor noise is a fundamental limiting factor in image restoration, hence the study of the characteristics of sensors is an important undertaking. Sensor noise data can be useful in two ways. First, it can be used for comparison of the relative effectiveness of various sensors so that the sensor which will produce the best signal to noise ratio in a given application can be used, or at least considered for use. Second, sensor noise data can be used in simulation studies whose purpose is to evaluate system performance.

Photographic film is the most widely used sensor for recording images at the present, and the studies reported here are concerned primarily with film. However, the use of an image intensifier to amplify the flux level of the image prior to recording on film is of current interest.

---

[6] J. L. Harris, J. Opt. Soc. Am. 54, 606, 1964.

When properly used in this manner the limiting noise properties are then those of the image intensifier. The image intensifier, therefore, is included in an experimental sensor comparison in Section 2.4.

2.1 Selection of Film on Basis of Published Data

There is a wide variety of films available covering many combinations of speed, granularity, contrast, spectral sensitivity, modulation transfer function, backing, and size. The choice of a film is usually partly dictated by the requirements of the particular application in mind. The choice of a film for a given application may not always be the optimum choice from the standpoint of image processing. In spite of this it is still important to know how to choose the optimum film solely on the basis of maximizing the success of image processing techniques. This section of the report will present an attempt to determine the effectiveness of various films in a basic image processing problem using available published film data.

2.1.1 Criteria for Selection

The criteria for selection of the optimum film is based upon a hypothetical optical system whose purpose is to record with the least error possible the relative illuminance (or irradiance) values of an image. The exposure time and the entrance pupil of the system are fixed so that the total light energy available for exposing the film is fixed. The size of the image, however, can be varied at will by inserting lossless lenses to magnify or minify the image. The recorded image is to be scanned by an aperture whose width is some fixed fraction of the width of the image. Consider the image formed by the basic optical system itself and let the

exposure at a reference point on the object be E_0 and the required size of the scanning aperture be d_0. The exposure is expressed in lumen-sec/m^2 or (joules/m^2 in radiometric units) and is a flux-time per unit area (or energy per unit area) quantity. The insertion of additional lenses to obtain different image sizes results in exposure values of

$$E = \frac{E_0}{M^2} \tag{15}$$

and effective scanning aperture sizes of

$$d = M d_0 \tag{16}$$

where M is the magnification due to the additional lenses. To determine the optimum film to be used in recording this image, a magnification is chosen for each film which results in the proper exposure of that film at the reference element. Then each film is used as a photometer to measure the relative exposure of the reference element. This is done by measuring the density of the film at the reference element and obtaining the corresponding E value from the film characteristic curve. The relative accuracy with which this measurement can be made is the quantity which is used to select the best film.

If, for a given film type, the exposure is measured many times by this method a distribution of exposure values would be obtained. The inability to obtain the same value for each repetition of the experiment would be due to the granularity of the film. The mean of the measured values would be approximately E and the standard deviation, σ_E. A quantity of interest would be σ_E/E since this is a measure of our ability to measure small variations of the actual exposure.

2.1.2 Derivation of the Figure of Merit

If $\sigma_E \prec\prec E$ then it can be shown that[7]

$$\frac{\sigma_E}{E} \approx \frac{\sigma_D}{\gamma \log_{10} e} \tag{17}$$

where σ_D is the r.m.s. density granualrity value of the film at the density corresponding to E and γ is the slope of the characteristic curve at the same density. If the scanning aperture is large with respect to the film grain size, σ_D is related to the aperture size by[8]

$$\sigma_D \approx \frac{G\, d_m}{d} \tag{18}$$

where G is the r.m.s. density granularity value measured by an aperture of size d_m. Kodak usually publishes the value of G for their films measured at a net density value of 1.0 above base density and with an aperture diameter of $d_m = 48\mu$. Since this density value is the only one at which G is specified in the published data, an arbitrary assumption will be made that the exposure which produces a net density of 1.0 is the optimum value. Then, from the published characteristic curve data, this "optimum" exposure can be found.

Since the required E value for a given film is now known, the magnification required to produce the optimum exposure of the reference point on the film can now be found from Eq. (15).

---

[7] F. S. Weinstein, J. Opt. Soc. Am. 59, 108 (1969).

[8] G. C. Higgins and K. F. Stultz, J. Opt. Soc. Am. 49, 925 (1959).

$$M = \left(\frac{E_0}{E}\right)^{1/2} , \tag{19}$$

which allows Eq. (16) to be written as

$$d = \left(\frac{E_0}{E}\right)^{1/2} d_0 . \tag{20}$$

Using the value of d in Eq. (18) gives

$$\sigma_D = \frac{G\, d\, m\, E^{1/2}}{E_0^{1/2}\, d_0} . \tag{21}$$

Substitution of Eq. (21) into Eq. (17) gives

$$\frac{\sigma_E}{E} = \left(\frac{d_m}{(\log_{10} e)\, E_0^{1/2}\, d_0}\right)\left(\frac{E^{1/2}\, G}{\gamma}\right). \tag{22}$$

The quantity $d_m / [(\log_{10} e)\, E_0^{1/2}\, d_0]$ is independent of the choice of film, assuming the G values are all measured with the same aperture. The quantity $E^{1/2}\, G/\gamma$ can be used as figure of merit for comparing various films. Define F as the figure of merit:

$$F = \frac{E^{1/2}\, G}{\gamma} . \tag{23}$$

This is the quantity which will be used for the comparison of the different films.

2.1.3 Application to Commercial Films

The quantity F has been computed for a wide variety of films ranging from the very slow, fine grain films to the very fast, very grainy films.

All of the films are panchromatic with extended red response. The results are tabulated in Table 1. The results should be considered to be approximate values since the E and γ values had to be read from the small un-ruled graphs provided by Kodak.

Several interesting results should be noted. First, although the speeds of the films considered ranged over three orders of magnitude, the F values ranged only over a factor of 5.6. This result does not come as a complete surprise since we know that the speed and granularity of a film are inversely related. If a faster film is used the flux density required is decreased, allowing the image to be made larger. When scanning the image a larger aperture can be used which offsets the effect of the increased granularity. The second point to be noted is that the maximum and minimum values occurred for the same film, i.e., 2485 High Speed Recording Film. The difference was due to a change in the method of developing the film. This result implies that either development methods are a major factor in the determination of F or that the analysis is not giving a true picture of the performance of the film. The latter is probably true since the assumption was made that the optimum exposure for each film was that which produced a net density of 1.0. No consideration was given to how G and γ vary as a function of exposure. To do the job properly would require the selection of an exposure which minimized $E^{1/2}\, G/\gamma$ as a function of E.

2.3 Noise Measurements on 3404 Film

To illustrate the variation of σ_E/E as a function of E, noise characteristics of 3404 film have been measured at the Visibility Laboratory.

TABLE I

FIGURE OF MERIT FOR SELECTED FILMS

TYPE	DESCRIPTION	DEVELOPMENT	SPEED	G	γ	E	F
3404	High Definition Aerial	D-19,8min,68F	1.6+	.0097	2.6	6.0×10^{-1}	2.9×10^{-3}
SO-243	Special High Definition Aerial	D-19,8min,68F	1.6+	.0074	2.3	6.3×10^{-1}	2.6×10^{-3}
SO-206	Special Aerial	D-19,8min,68F	6.0+	.014	2.2	1.7×10^{-1}	2.6×10^{-3}
3400	Panatomic-X Aerial	D-19,8min,68F	20+	.020	1.9	4.1×10^{-2}	2.1×10^{-3}
SO-136	Panatomic-X Aerial	D-19,8min,68F	20+	.020	2.2	4.2×10^{-2}	1.9×10^{-3}
3401	Plus-X Aerial	D-19,8min,68F	64+	.035	2.0	1.8×10^{-2}	2.3×10^{-3}
8401	Plus-X Aerocon	D-19,8min,68F	80+	.034	2.0	1.4×10^{-2}	2.0×10^{-3}
5425	Super-XX Aerographic	D-19,8min,68F	100+	.037	1.4	1.7×10^{-2}	3.4×10^{-3}
2405	Double-X Aerographic	DK-50,8min,68F	125+	.036	1.4	1.5×10^{-2}	3.2×10^{-3}
8403	Tri-X Aerocon	D-19,12min,68F	200+	.048	1.3	8.9×10^{-3}	3.5×10^{-3}
2485	High Speed Recording	D-19,12min,75F	5000*	.060	2.6	2.7×10^{-3}	1.2×10^{-3} (Min Value)
2485	High Speed Recording	MX642-1,1min, 98F	1250*	.049	.77	1.1×10^{-2}	6.7×10^{-3} (Max Value)
2485	High Speed Recording	MX642-1,2min, 98F	8000*	.068	1.9	1.6×10^{-3}	1.4×10^{-3}
2475	Recording	DK-50,8min,68F	4000*	.049	1.0	4.7×10^{-3}	3.4×10^{-3}

Speed — + denotes Aerial Exposure Index; * denotes ASA Speed Index.

G — The r.m.s. density granularity value specified by Kodak x 1/1000. The value given by Kodak is described as "1000 times the standard deviation in density produced by the granular structure of the material when a uniformly exposed and developed sample is scanned by a densitometer having an optical system aperture of f/2.0 and a circular scanning aperture 48μ in diameter". In all cases this quantity is measured at a density 1.0 above the base density.

γ — The slope of the characteristic curve at a density of 1.0 above the base density.

E — The exposure in meter-candle-secs or lumen-secs/m^2 which produces a density 1.0 above the base density.

F — The figure of merit, $F = E^{1/2} G/\gamma$.

The measurements were made in the following manner. Uniform exposures were made by exposing the film with a Xenon flashtube filtered with a .69 micron narrow band filter. Neutral density filters were used to vary the flux level over a wide exposure range. The film was developed in D-19 for 5 minutes with continuous agitation. The resulting transparencies were scanned over an array of 10 x 10 picture elements at each density level using the microscope scanner described in Section 4.2. Scanning apertures of 2.2 and 1.0 microns were used. For each of the 10 x 10 arrays the sample mean, $\bar{T}$, and standard deviation, σ_T, of the transmission values were computed. This was done for several sets of scans in order to get an indication of the reliability of the data. The results in the form of $\sigma_T/\bar{T}$ versus $\bar{T}$ are shown in Fig. 8 along with the system noise. The system noise was measured by turning off the stepping motors and defocusing the microscope to avoid any scanning of the film grain. While this data does not represent a significant error study of the measurements, the spread between data points and the low system noise indicates that the data is fairly reliable. It should be pointed out that film measurements are always dependent upon certain characteristics of the optical system used to make the measurements, particularly the numerical aperture of both the illuminating and collecting optics.

The raw data values from which curves A and D were obtained were converted into exposure values by use of an analytic formula used to represent the film characteristic curve, which is shown in Fig. 9.

Thus for each original uniform exposure a 10 x 10 array of exposure values was computed. The sample mean $\bar{E}$ and standard deviation about this mean, σ_E, were computed. These data are shown in Fig. 10 along with an

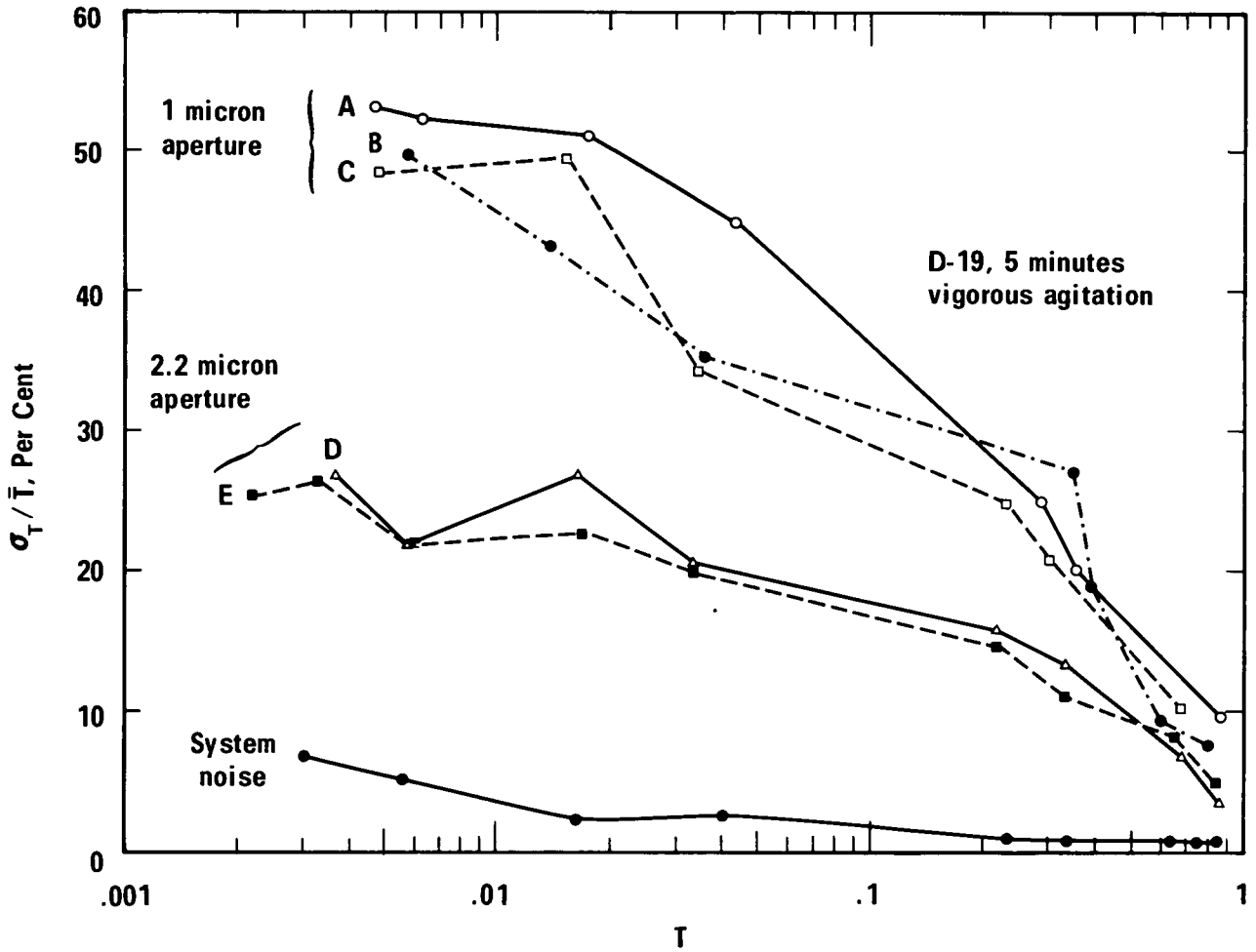

Fig. 8. $\sigma_T / \bar{T}$ versus $\bar{T}$ for 3404 film.

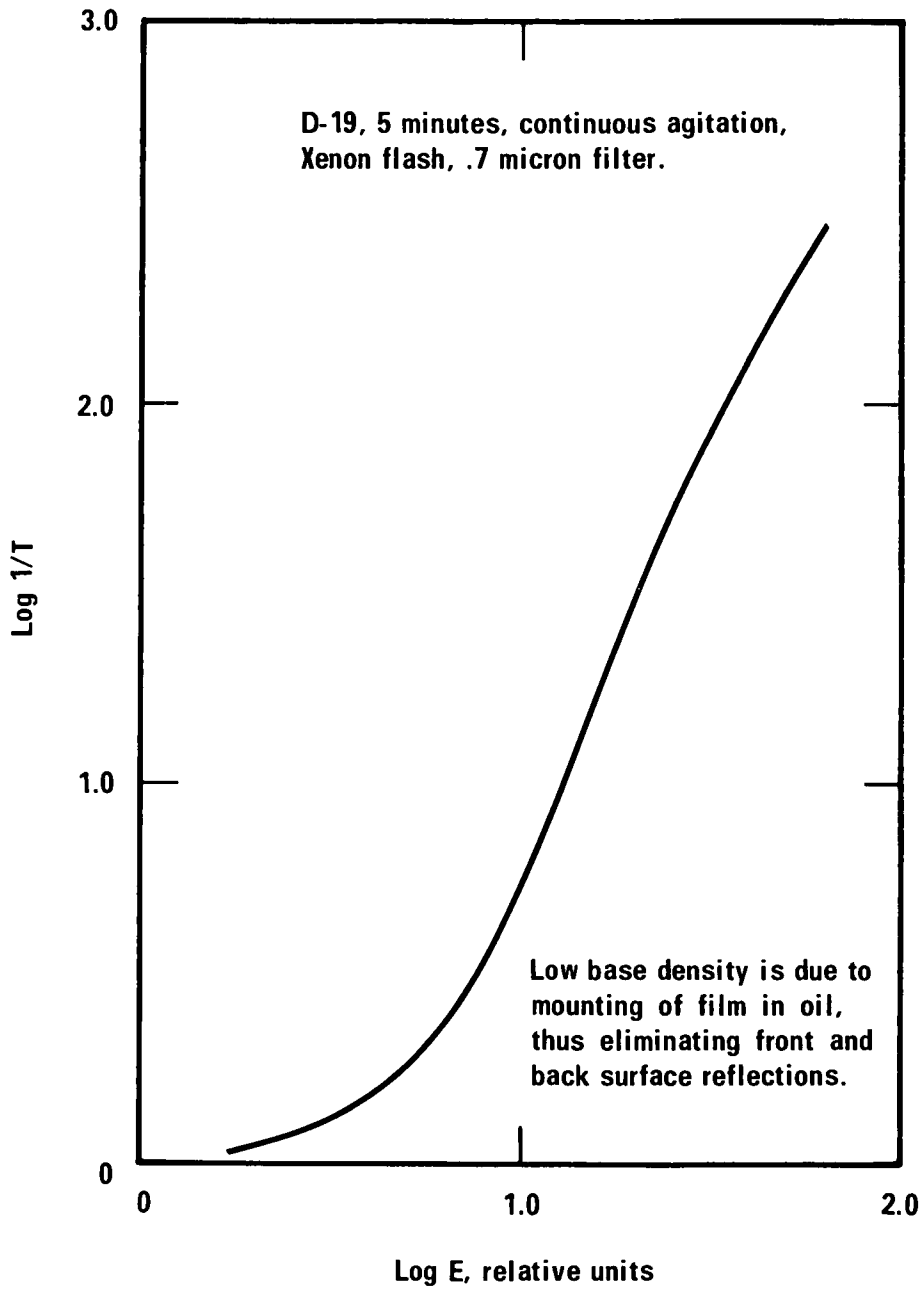

Fig. 9. 3404 film characteristic curve.

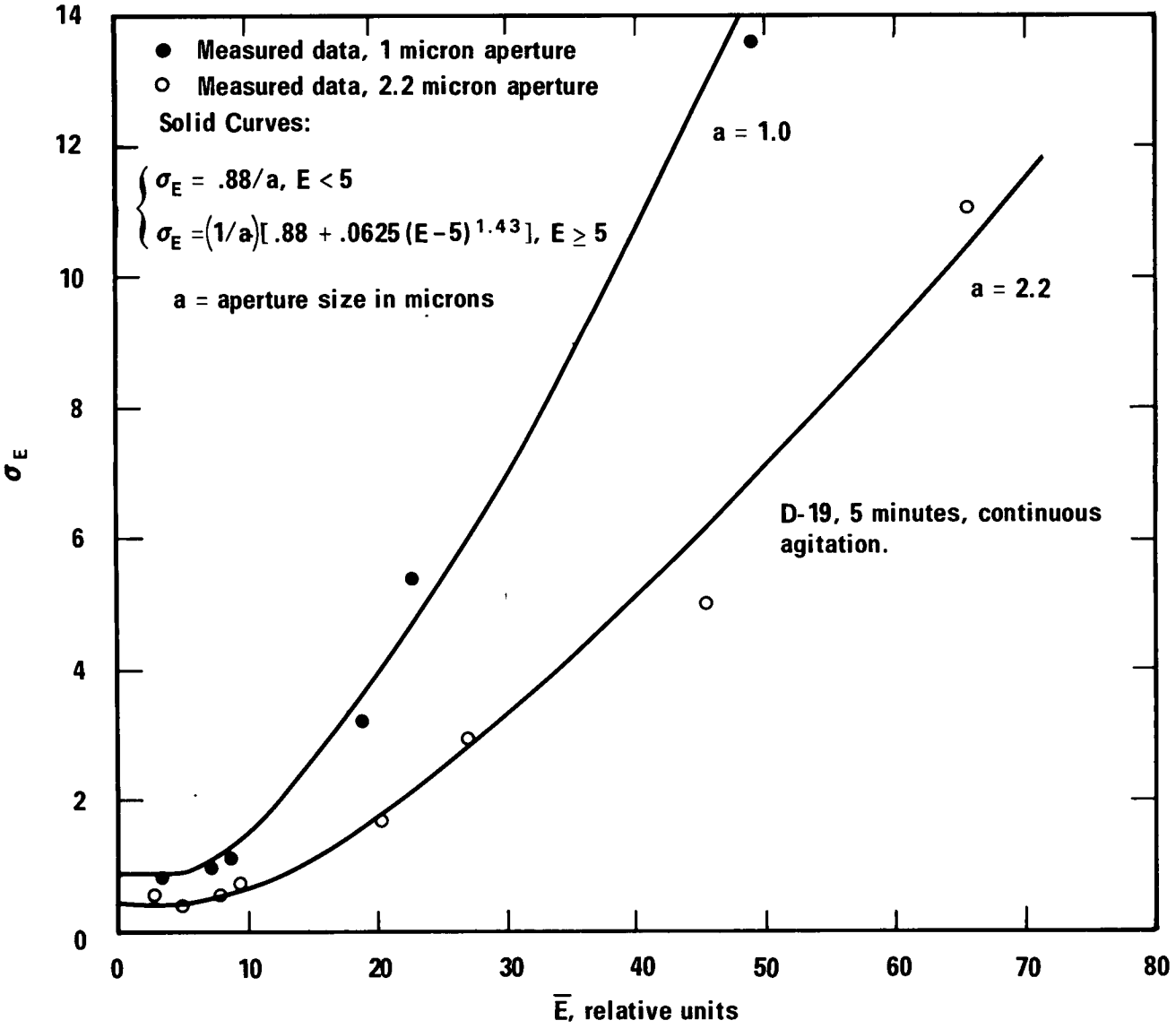

Fig. 10. σ_E versus E for 3404 film.

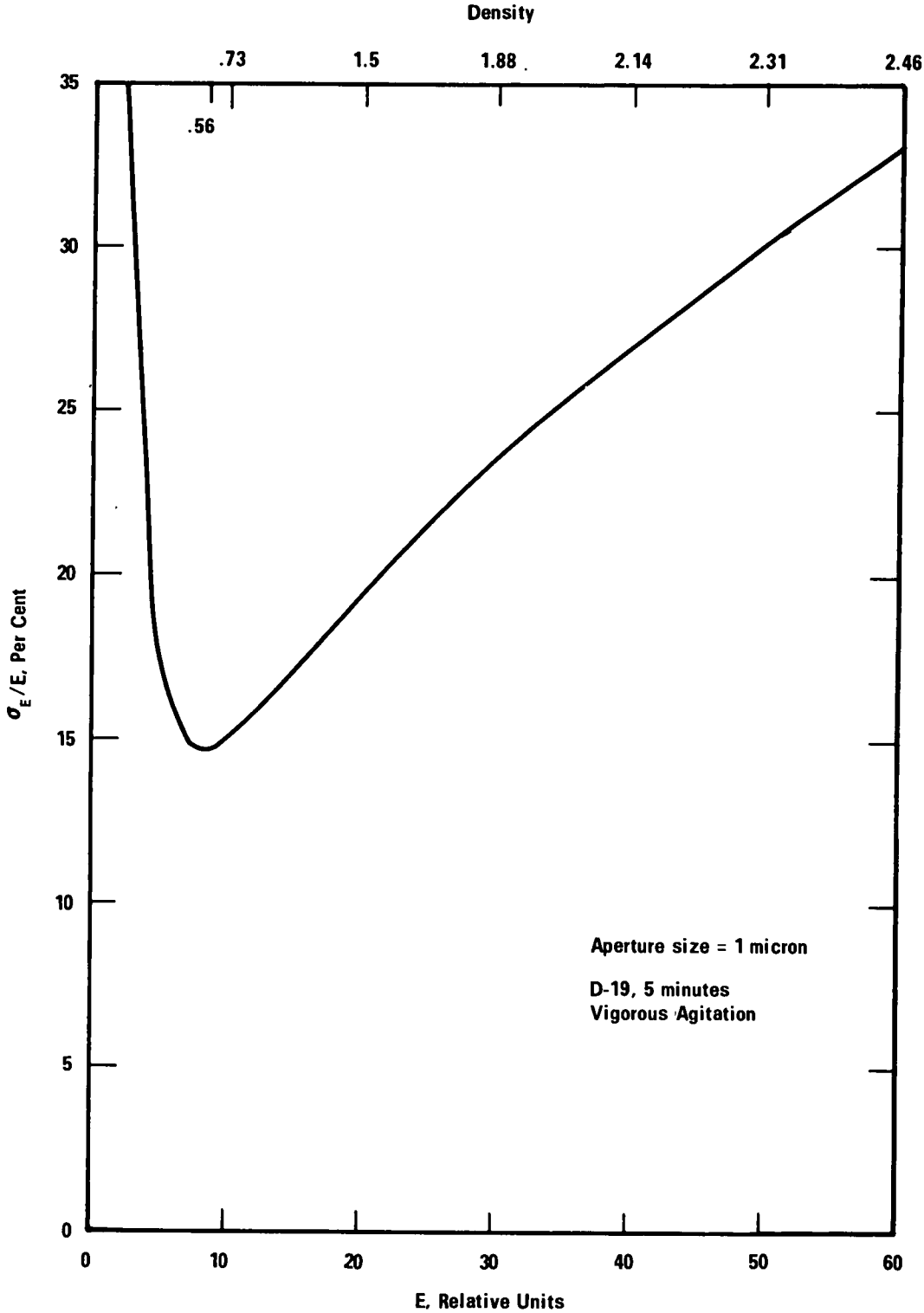

Fig. 11. σ_E/E versus E for 3404 film.

analytic curve which has been used to represent the data in simulation studies. Using this equation $\sigma_E/\bar{E}$ versus E has been computed for the one micron aperture. The results are shown in Fig. 11. This curve represents the ratio of the error in measurement of scene exposure to the true scene exposure as a function of the exposure.

Several interesting implications can be drawn from this curve. $\sigma_E/\bar{E}$ varies significantly as a function of $\bar{E}$. Therefore, expression of film gramularity at a specific film density is not sufficient to describe the noise characteristics of the film, a conclusion which was suspected in Section 2.2. The curve also demonstrates that the selection of an optimum exposure, especially from the standpoint of image processing, is a complex situation. Different parts of a continuous tone image will have different signal to noise values. The problem appears even more complex if the total amount of flux is fixed and some integrated signal to noise ratio is to be maximized by varing the size of the image. As the image size is varied the range of exposure values in the image changes. To maintain a constant resolution with respect to object space the scanning aperture size also changes, a change which is reflected in the scale of the ordinate of the σ_E/E curve. And finally the size of the point spread function of the film changes in size with respect to the image size.

2.4 Comparative Sensor Measurements

In Section 2.1 it was shown that selection of a film to minimize scene irradiance measurements in a flux limited case cannot be done on the basis of presently published film specifications. Section 2.3 demonstrated some of the measurements that would be needed for all films under consideration and pointed out the complexities of making the determination even when the basic data is available. This section will present an experimental approach to the problem.

2.4.1 Description of Experiment

A hypothetical problem was posed as follows: given a constant energy image whose size can be varied at will and the choice of four sensors: 3404 film, 3400 film, 2485 film, and a three stage S-20 image intensifier, which sensor will give the highest quality image? The choice of film covers the range from very slow to very fast speed indexes. The image intensifier was included because of its emergence in the past few years as a very sensitive detector.

An Ealing resolution pattern was used as the test object. It was illuminated by a microscope illuminator filtered with a narrow band pass filter with a band width of about .02 microns centered on .69 microns. A 2mm thick piece of diffuse plastic was placed directly behind the object to reduce coherence effects. An aerial image 1/10 of the object size was formed by the use of a 10X microscope objective which had a numerical aperture of .25. The theoretical frequency cutoff in this image was 700 cycles/mm. Over 600 cycles/mm were observed visually with the aid of a 20X objective microscope. The image plane of the 10X objective was taken to be the reference plane for the experiment. The 3404 film exposure was made at this plane. The film was held in a Richardson film transport mounted on a micrometer-driven plate. Rough focusing was accomplished by the use of a microscope positioned on the backside of the film, focused upon the film grains of sample piece of film. With the test film in place fine focusing was obtained by taking many exposures, moving the film along the optical axis to vary focus and perpendicular to the axis to separate the individual exposures. The exposures were made at 1/50 sec.. Several different runs were made on 3404 film, each at a different flux level to find the exposure level which produced the highest resolution. Once this

was found the total flux in the image was measured with a silicon photovoltaic cell. This total flux value then became the value used for all the other sensors.

Image size for the other sensors was changed by the use of various microscope objectives to magnify the primary image. In order to minimize spherical aberrations, microscope objectives must be used at their design working distance. For the available microscope objectives, including combinations of infinity-corrected objectives, this limited the possible magnifications to 2.0, 2.5, 5.0, 10.0 and 10.5. For all cases the effective numerical aperture of the objectives following the primary 10X objective were equal to or greater than .25 . Thus all were theoretically capable of passing all spatial frequencies passed by the first 10X objective. Of course some attenuation probably occurred as the result of aberrations. For this reason this test should be judged principally in terms of the appearance of the noise characteristics of the images rather than the limiting resolution. For 3400 film the best exposure was obtained at M = 2.5, for 2485 film at M = 10.5 . The image intensifier required a magnification of 70. This was obtained by the use of an infinity corrected objective. In this case the image was sufficiently far from the objective that the spherical aberrations were negligible. The output image from the image intensifier was recorded on 2485 film with a 1:1 camera. The image size was sufficiently large on the film that the film grain was relatively small. In order to reduce background buildup on the image intensifier the camera shutter was opened briefly before the exposing shutter on the illuminator and closed immediately after the exposure.

2.4.2 Experimental Results

The results of this experiment are shown in Fig. 12. Of the films, 3404 produced the best results in terms of signal to noise ratio and also in terms of the limiting resolution with respect to object space. However, as pointed out previously, limiting resolution should not be used as a criterion. Between the image intensifier and 3404 film, the image intensifier produced the best image. The implication is that the image intensifier is potentially a useful sensor for applications presently using 3404 film. However, there are at least two major factors to be considered in such an application. First, assuming 3404 film would be used in the primary image plane of an optical system, additional optics would be required to provide a magnified image for the image intensifier, resulting in a loss of flux and a longer optical path length. This magnification is necessary to make the image large enough to overcome the effects of the low resolution of the image intensifier so that the object space resolution is maintained. Second, the requirement for a magnified image results in a reduced field of view. Assuming that the film and image intensifier have about the same useful area, the field of view would be reduced by the magnification. For this experiment the magnification was 70. The tube used is an experimental device manufactured several years ago. Current types quite possibly have better resolution and would require less magnification.

Another factor which should be considered is spectral response. This experiment was made at wavelengths within a narrow band (about .02 micron) at .69 microns. This is at about the peak of the spectral sensitivity of 3404 film, according to Kodak publications. The spectral quantum efficiency

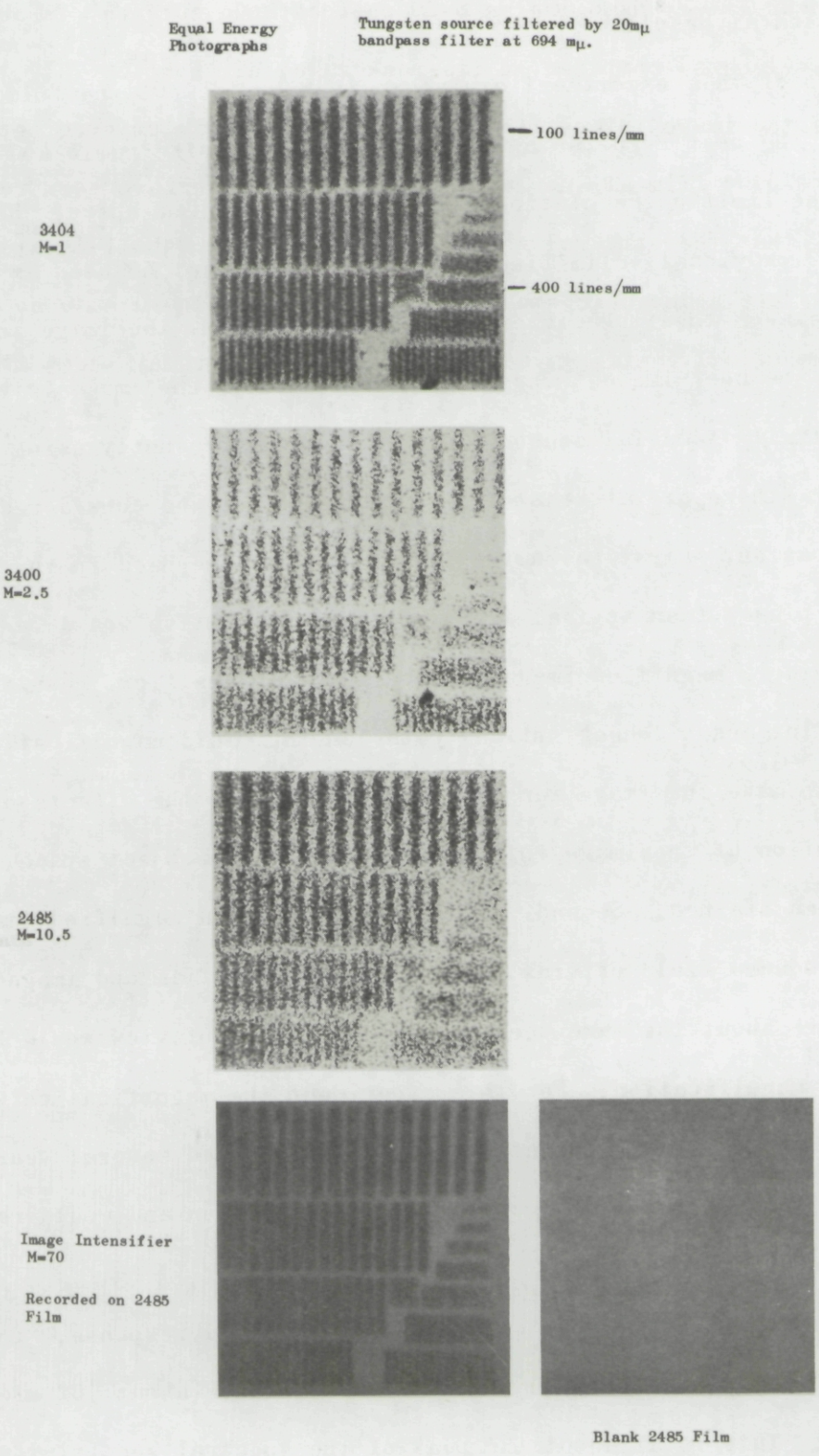

Fig. 12. Comparison of sensors for equal energy input.

of the image intensifier, assuming an S-20 photocathode surface, is about 2.5% at this wavelength, compared to its peak value of about 20% at .4 microns. Thus the image intensifier might be expected to do even better in comparison to 3404 film at shorter wavelengths. There have been reports, however, that the spectral sensitivity curves for 3404 film are not accurate. Therefore a thorough study of the subject would have to be made to determine the relative effectiveness of the two sensors at shorter wavelengths.

3.0 THE IMAGE PROCESSING COMPUTER SYSTEM

3.1 Introduction

A great deal of image processing studies have been done in the past on the CDC-3600 computer at the University of California, San Diego, computer center. These studies accomplished two major points. First, successful restorations of degraded images demonstrated the feasibility of image processing. Second, image processing on real images was found to usually involve several variables, some of which were not known numerically and had to be varied to optimize the restored image. Experience with the closed shop operation at the campus computer center led to a conviction that a computer facility in which the experimenter could control the image processing steps on-line was a needed tool for the research. To this end an IBM 1800 computer system was installed and put into operation in October 1967 at the Visibility Laboratory. This section briefly describes the computer system and programs.

3.2 Configuration of the Computer System

The Visibility Laboratory computer installation at the Visibility Laboratory, shown in Fig. 13, is an IBM 1800 system. The particular configuration of this machine is characterized by the following features:

a) 32K 16-bit word core size, core cycle time of 2 microseconds,

b) One 1442 card reader (300 cards/minute)

c) One seven-level 2401 magnetic tape unit,

d) One 1810 2-drive disk unit,

e) One 1443 line printer (150 lines/minute),

f) One digital-to-analog converter (DAC),

g) One digital/analog output device (DAO),

h) One 1816 typewriter/keyboard.

3.3 Program Philosophy

Image processing at the Visibility Laboratory is now being accomplished through the use of a computer program regarded as a second-generation image processing program. The system is characterized by its flexibility in the sequence of executing stored programs, and by the variety of image processing operations.This contrasts with the first generation program philosophy of leading the investigator along a programmed path of computations with "windows" inserted at key points to allow the user to examine intermediate results. These periodic evaluations allowed the user the opportunity to make judgements concerning the use of optional paths that might be taken at that point in time.

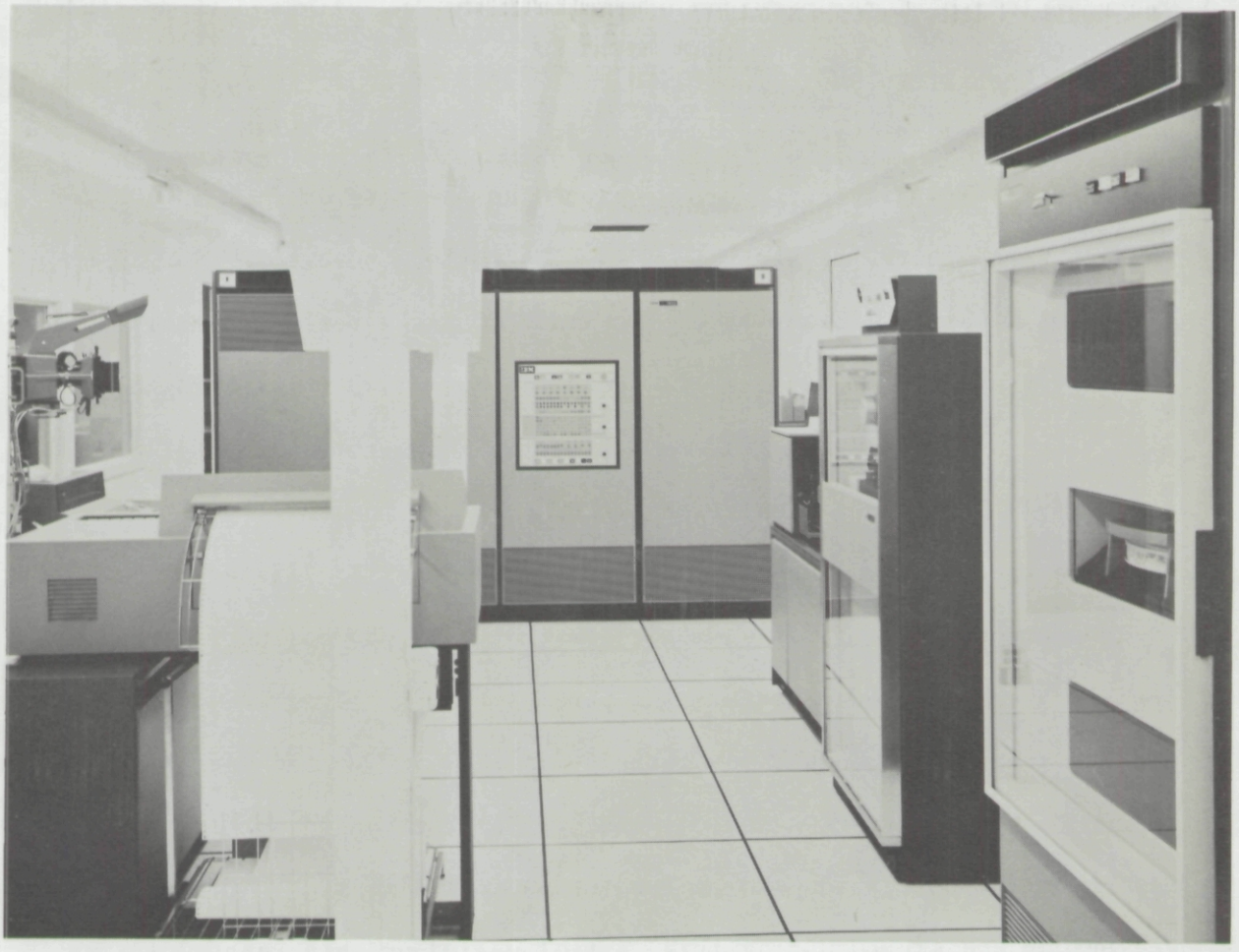

Fig. 13. The IBM 1800 Computer at the Visibility Laboratory.

In contrast to the earlier philosophy, the present system requires the user to make a decision concerning the choice of a new matrix operation upon completion of the previous operation. The investigator is presented with a list of image processing operations and is at liberty to select any one of them to come into core for execution. The various operations are, in reality, discrete programs stored on the program disk (drive zero). These programs have, in general, a task to perform on a matrix or in a region of a matrix. Examples of the kinds of tasks performed are: 1) the reading of a matrix into core via the card reader; 2) multiplying one matrix by another matrix; 3) computing the Fourier transform of a matrix; 4) displaying a matrix on a CRT. At the present time there are 72 of these operations. The most frequently used ones are listed in Table II.

When execution is first commenced in the image processing program, certain user-supplied environmental parameters are stored in the COMMON storage area. This data is concerned with the size of the user's matrix, the number of matrix rows and columns, ID information concerning the nature of the processing, and picture count initialization. Other parameters are set up and stored during this initial period and are related to the particular computer system being used. Such information as I/O device unit numbers and maximum matrix size is in this category.

After environmental setup has been accomplished, the user is then in the position of being able to arbitrarily select an operation, wait for its completion, then proceed to another operation and so on until his specific image processing task is completed. The program is organized so that a controller program is assigned the responsibility of performing

TABLE II

IMAGE PROCESSING COMPUTER OPERATIONS

1. Card data input.
2. Disk-core input/output.
3. Characteristic curve applied to matrix.
4. Fourier Analysis of matrix.
5. Matrix shifts (12 options)
6. Transfer functions (35 options)
7. CRT picture of matrix.
8. Add two matrices element by element.
9. Subtract " " " by " .
10. Multiply " " " by " .
11. Divide " " " by " .
12. Moduli and phase from complex coefficients
13. Print all or part of matrix
14. Punch all or part of matrix
15. Clip or rectify matrix.
16. Store constant in a matrix section.
17. Look-in on matrix element.
18. Roll-off functions (5 options).
19. CRT graph any column or row.
20. Logs of matrix.
21. Antilogs of matrix.
22. Generate random numbers with normal distribution.
23. Statistical Analysis of matrix.
24. H + D curve fit.
25. Matrix edge smoothing.
26. Center of gravity computation and shift.
27. Complex co-efficients from amplitude and phase.
28. Ring structure find.
29. Bar structure find.
30. Integrate along column or row.
31. Disk to tape dump.
32. Tape to disk dump.
33. Image derivative.
34. Min/Max of matrix.
35. Rotate matrix.
36. Least squares filter.
37. Matrix magnify.
38. Go to card mode.
39. Go to typewriter mode.

disk I/O at the beginning and end of an operation, calling on the various keyboard mode, card mode or memory mode routines, and fetching the appropriate program from the disk to execute the requested operation.

3.4 Core Usage

The monitor system used is the IBM 1800 TSX (time-sharing executive system), non-process mode. Approximately 6K words in core are required to contain this program. Of particular value to Visibility Laboratory usage of the 1800 is the ability of the TSX monitor to compile programs in core image format and to store them on the disk as permanent disk residents. These stored programs can be fetched from the disk into core for execution via the Fortran CALL LINK statement. Minimum time is spent bringing a program into core for execution, since a program's core addresses were previously assigned at coreload build time, i.e., when the program was first stored on the disk.

A significant portion of core, 18K words, is devoted to the COMMON storage area. COMMON is an area in core reserved for data storage and can be referenced by any program which is resident in core at a given time. The COMMON area differs from a program's individual data storage area (DIMENSION area) in that when a particular program is overlayed in core by another program, the data in COMMON is preserved, whereas the data local to a program being overlayed is not preserved. Along with the need to store a complex image data matrix (16K words) is the need to store numbers related to executing the various image processing programs. These numbers are of two kinds and occupy 2K of core. Integers thought of as operation parameters are numbers of the first kind. They serve to control the flow of logic within the program according to choices made by the user,

and to direct matrix I/O to and from user-determined disk files. Numbers of the second kind are real (floating point) numbers used as data parameters in arithmetic computations, e.g., coefficients in a polynomial expression used in generating a characteristic curve.

A space of approximately 8K is left as space available to the main program and its associated subprograms comprising the coreload. Because a large part of core is devoted to COMMON, frequent use is made of the TSX monitor's ability to load subroutines into core during execution of the calling program: the subroutine can be classified as a type to be loaded at call time and is then not included in the coreload at coreload build time. This, in effect, increases available core space and allows a much larger coreload to be executed than the 8K coreload space mentioned above would indicate.

In summary core usage is as follows:

System Monitor	6K
Common	
Image Data	16K
Operation Parameters	2K
Operation Program Coreload	8K
	32K

3.5 The Image Processing Data Matrix

The image processing system written for the 1800 has, as a fundamental unit, a double 64 x 64 element matrix. One of the matrices contains the real parts of a complex array; the other contains the corresponding imaginary parts. The computer uses two 16 bit words to store one floating point number in core. Two 64 x 64 element matrices therefore requires 16,384

computer words to contain them. This represents the use of one-half of the available core space. The elements in both of the two matrices are stored in consecutive locations in core for efficient FORTRAN indexing, i.e., the real and imaginary parts are each represented as a solid block of numbers. The image processing program has the capability of storing the matrix on magnetic tape or disk as permanent records or files. Approximately 800 64 x 64 real matrices can be stored on a 2400 foot tape, and a total of 63 can be stored on the two disk drives: 4 on drive zero and 59 on drive one. (The disk cartridge mounted on drive zero contains IBM and image processing programs and therefore has minimum space left over for the storing of data matrices; the disk on drive one is devoted entirely to the storing of matrices).

3.6 Modes of Computer Operation

3.6.1 Keyboard/Typewriter Mode

There are three modes of operation the investigator can use while performing computations. The first of these modes is the Keyboard/Typewriter mode. An operation arbitrarily selected from the list of image processing operations is entered on the keyboard in response to "SLCT OP=XX" (which stands for "select operation") on the typewriter carriage. The typewriter then types questions pertinent to the particular operation requested. The investigator answers these questions on the keyboard and causes execution of the operation to commence by pressing the end-of-file (EOF) key. When the operation is completed, the message "SLCT OP=XX" is again presented and the investigator can make another selection from the list of image processing operations.

3.6.2 Card Reader Mode

This mode is similar to the keyboard mode in that the investigator must supply responses to questions related to the requested operation. These responses, however, instead of being entered at the keyboard, are entered on punched cards to be read through the card reader. These instruction cards may be stacked in the card reader so that many operations can be serially executed without the need of further operator intervention or presence. The nature of the investigation determines which of the two modes described above is used. If the work is predominately exploratory, the keyboard method is favored because of its flexibility. If a production run is to be made, the card reader mode is generally used; the use of this mode usually implies that the user knows, in advance, the sequence of operations needed and does not need to observe intermediate results before proceeding to a new operation.

3.6.3 Memory Mode

A third operating method, known as the memory mode, is an extension of the card reader mode. A sequence of card instructions is read through the card reader as in the card mode scheme. Program execution, however, does not take place following the reading of a card (or cards) for an operation. Instead, this card information is stored in a table in core memory. In using this sytem the card information from the entire set of cards loaded in the card reader is stored sequentially in this table where it remains ready to be interpreted by the image processing supervisor program when execution is called for. This operating scheme has as its unique feature the ability to execute this memory mode table repeatedly. In building the table, the operator, by following rules governing the make-up

of the card deck, can cause certain of the data parameters used by some of the operations to be regularly incremented during successive passes through the table. The number of such passes through the table is specified by the investigator prior to the start of execution.

4.0 IMAGE PROCESSING EQUIPMENT

4.1 Introduction

In general, active image processing involves the operations of scanning, computer processing, and output display. The scanners may be further subdivided into the categories of mechanical stepping or electronic stepping. Two equipments exist for performing mechanical stepping, the Object Plane Scanner and the Microscope Optical-Mechanical Scanner. Two control and recording systems are vailable to drive these scanners. These are the Punched Card Recorder and the Magnetic Tape Recorder. Either of these units can be employed to control either of the optical-mechanical scanning units. The former digitizes at a fairly slow rate with a high degree of accuracy onto punched cards. The latter records on magnetic tape at a faster rate but with a somewhat reduced accuracy. Working in conjunction with these two units is the Remote Scanning Console which serves to accurately position the scanning heads for setup before the actual scan begins. Both recorders have the capability for generating polaroid prints either from magnetic tape or from punched cards. This is essentially an off-line operation and was employed to a greater extent when the computer processing was done at the campus computer center.

The Microscope Flying Spot Scanner and the Image Dissector are both electronic scanners. These two units are currently under development. The Microscope Flying-Spot Scanner is essentially a flying spot scanner system coupled to a microscope. With it, micron step sizes should be realizeable. The Image Dissector is employed for non-photographic scanning, such as models subjected to accurately controlled lighting conditions. Both of these scanners will be under direct computer control, in that both the digitization and stepping will be accomplished via the 1800 analog-to-digital converter and digital-to-analog converters respectively. There is an advantage here in that a scan operation can be inter-mixed with processing operations on the computer should the image processor so desire.

The 1800 Refresh Display System* serves as the output device whereby the processed material is observed. For an immediate look at the result a small black and white TV type presentation is available. A hard copy of the results can also be made on polaroid or 16mm film. A storage display is available for curve plotting. Certain simple operations can be performed on the picture matrix by the system such as invert, clip, rectify and shift. The unit has its own core storage so that the computer is essentially free to perform other operations once a data transfer has been accomplished.

The last subdivision in this section of the report has been devoted to a description of the research equipment. Experimental flying spot scanners and refresh displays had been built up and operated as an initial step before the design of the operational models was attempted. The various picture generation techniques were also experimentally tested prior to actual construction and installation.

---

* This system was developed under other funding. It is described in this report because it is an integral part of the over all image processing facility.

4.2 The Microscope Optical-Mechanical Scanner

Two optical-mechanical scanners are currently in use. One of them, the Object-Plane Scanner, has been described in detail in a previous report.[9] In this unit scanning is accomplished by a stage which is driven horizontally and vertically by pulsed incremental motors. The step size is 100 microns. The film to be scanned is mounted on the stage and imaged on a fixed sampling aperture. While this scanner exhibits excellent field uniformity characteristics, it is limited to one step size. The Microscope Optical-Mechanical Scanner overcomes this limitation.

4.2.1 Description

The basic optics of the Microscope Optical-Mechanical Scanner, shown in Fig. 14, is provided by an American Optical Microstar microscope. Illumination of the object is provided by an American Optical Ortho-Illuminator which uses the principle of Koehler illumination. The object to be scanned is placed in the specimen plane of the microscope. Any of five objectives can be used, according to the sampling resolution required. The objective powers are 4X, 10X, 20X, and 45X and 100X (oil immersion). The numerical apertures of these objectives are, respectively, .12, .25, .50, .66 and 1.25. The collimated flux bundle leaving the objective lens travels up to a Dual-Viewing attachment. In this device the beam is divided into two parts. One beam continues upward where it enters the standard binocular head. This is used for viewing purposes. The other beam travels horizontally into a standard monocular telescope, used without the eyepiece. The magnified image is formed in the focal plane of the telescope. The scanning aperture is placed in this plane. The scanning aperture is driven by a scanning

---

9 J. L. Harris, Scripps Institution of Oceanography report 63-10, 1963.

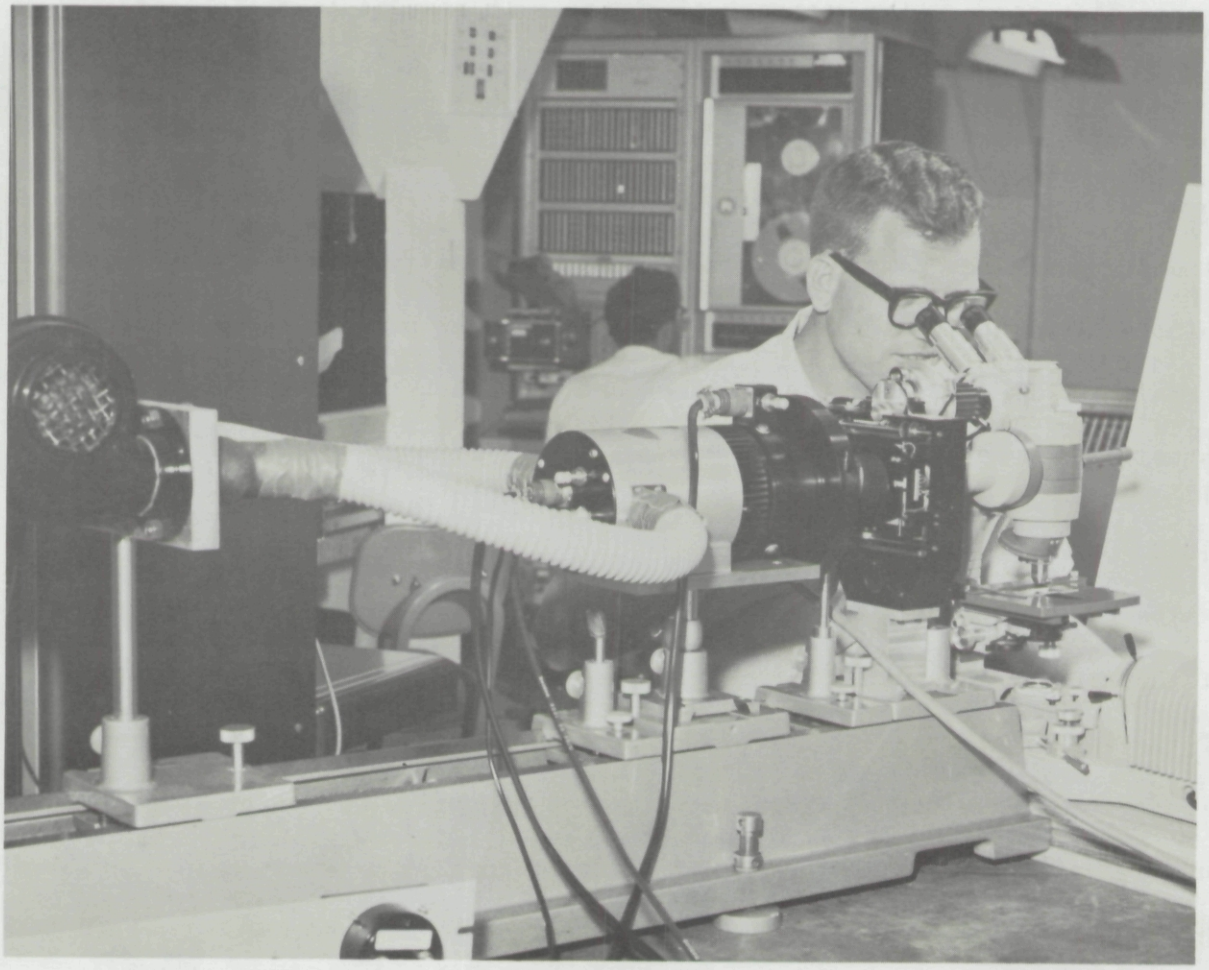

Fig. 14. The Microscope Optical-Mechanical Scanner.

head similar to that used in the Object Plane Scanner. However, this head employs a gear train which allows a choice of 100, 75, 50, and 25 micron step sizes. The scanning step size with respect to the object is determined by dividing the mechanical step size by the objective power. For example, the 100 micron step size with the 45X objective would result in an object plane step size of 2.2 microns. A field lens is located behind the scanning aperture. This images the objective stop onto the photocathode of a thermo-electrically cooled multiplier phototube. The electrical output of this phototube can then be sent to either the punched card or magnetic tape recorder console.

4.2.2 Characteristics

The resolution of the scanner is determined by the inherent resolution of the microscope and the size of the scanning aperture. The combination of the illuminator and microscope produces an instrument capable of very high resolution. For a diffraction limited objective the point spread function with respect to the object plane is an Airy disk of radius $.61\lambda/n \sin\theta$, where λ is wavelength, n is the refractive index of object space, and $\sin\theta$ is one half the acceptance angle of the objective.[10] The quantity $n \sin\theta$ is also known as the numerical aperture (N.A.) of the objective. The highest spatial frequency, or cutoff frequency, contained in the point spread function is $2n \sin\theta/\lambda = 2$ N.A./λ . For $\lambda = .55$ microns the f_{co} values for the 4X, 10X, 20X, 45X, and 100X objectives are, respectively, 436, 910, 1820, 2400, and 4360 cycles per millimeter. Because the lenses are not perfect the useful cutoff frequencies are probably less than the theoretical. Measurement of the actual optical transfer function would be a very difficult

[10] Born and Wolf, Principles of Optics, (MacMillan Co., New York, 1964), p.424.

task. Visual tests have shown that a 1000 line/millimeter square wave pattern is easily resolved with the 20X objective. This combined with the fact that film grain noise will usually prevent the use of spatial frequencies above 500 cycles/millimeter indicates that the resolving capabilities of the microscope are completely adequate. The highest spatial frequency, f_{max}, sampled in the scanning process is M/2a where M is the objective power and "a" is the distance between samples. For M = 100, a = 25 microns, f_{max} = 2000 cycles/millimeter. Again this far exceeds any needed value. In practice the 100 micron step size is usually used. Thus the values of f_{max} for the various objectives are 20, 50, 100, 225, 500 cycles/millimeter. The optics behind the scanning aperture do not affect resolution.

The field illumination uniformity of the microscope has been found to be strongly dependent upon the objective used, indicating that the non-uniformity lies in the illuminating optics rather than the collecting optics. Typical field variations, defined as (maximum-minimum)/average, are: 100X-5%, 45X-5%, 20X-7%, 10X-25%, 4X-50%. While the uniformity for the 100X, 45X and 20X objectives is probably adequate, there may be cases for the 10X and 4X objectives where the uniformity is not satisfactory. In such cases a no-object scan can be made to document the field non-uniformity. This data can then be used to correct the scanned data of interest.

The scanning head is capable of a 128 x 128 scanning format. When the head is properly loaded backlash is negligible at all step sizes, both horizontal and vertical.

The signal to noise ratio of the output of the scanner is a function of many variables: the objective, the amount of objective aperture used, the scan aperture size, the multiplier phototube characteristics; and the sampling time of the analog to digital recorder. Under the following conditions a signal to r.m.s. noise ratio in the range of 100 to 200 is typical: illuminator on "high", first diffuser of illuminator in, 2/3 of objective diameter used, no color filter; 100 micron aperture; EMI 9502S multiplier phototube with 100K load resistor, high voltage adjusted to give .5V load voltage; .1 second integration time. The signal to noise ratio varies slightly between objectives due to the difference in total flux transmitted by the different objectives. The signal to noise value stated represents that which would be obtained without film. As a film is scanned the regions of nearly unity transmission will exhibit this signal to noise ratio, approximately. Areas of less transmission will exhibit values of approximately the stated value multiplied by the square root of the transmission.

In general this scanner has been found to be a very reliable and useful research tool.

4.3 The Image Dissector Scanner

4.3.1 Description

The image dissector is a device used for conversion of optical images into electrical signals. Cylindrical in shape, 2.5" in diameter, and 12" long, the tube has a plane receiver end upon which incident light flux is focused by an objective lens. The inner glass surface of the receiver end has a semi-transparent photosensitive film, the photocathode. An electron

image is formed by the photons incident on the photocathode; this image is accelerated toward and focused at an aperture plane by the necessary electron optics of the tube. At the aperture plane all photo-electrons are collected except the few that arrive at the aperture opening. These pass through the aperture and enter into an electron multiplier or dynode string which serves as the tube's internal amplifier. The anode element collects the resulting secondary electrons and is the signal element of the dissector tube.

The scanning operation is accomplished by magnetically deflecting the electrons as they pass from the photocathode to the aperture plane. Actually the focused electron image is moved as desired across the stationary aperture. The size and shape of the aperture is fixed, but can be specified at will when the tube is initially fabricated. Appropriate deflecting coils and a focusing coil must be mounted about the tube to effect the above described operation.

Two types of image dissector tubes have been used in our work to date. The first tube used was the Westinghouse WL-23111. Much useful experience and information was obtained working with this tube type, but although two units were used, fabrication deficiencies in both necessitated our choosing a second tube type, the ITT F4052, for our present scanner.

Much of the operational data to be cited as part of this writing was obtained with the WL-23111 tubes, but because the characteristics quoted are largely properties of the system's supporting circuitry and mechanical adjuncts we feel safe in quoting them. This attitude is reinforced by our experience in operating the new F4052 tube; this unit is simpler to set up and operate and is more stable with respect to set up than was the WL-23111.

Hence, operation of the present image dissector scanning system can be taken to be at least as good as herein quoted unless otherwise stated.

4.3.2 Characteristics

Table III lists the parameters indicative of the operational capability of the image dissector scanner. All measurements were made for a 90 x 90 step scan covering the central .60" x .60" of the photocathode. The photocathode current was held at 1.0 microampere. The lens used as an objective was a Bausch and Lomb Baltar, F:2.3, 100mm.

TABLE III

IMAGE DISSECTOR OPERATIONAL PARAMETERS

Parameters		Conditions
1. Signal/Noise:	312	At 1.0μA photocathode current and stepping rate = 60 steps/second.
2. Positional Stability:	> ± .60%, (± 1/2 step max.)	Over a 40 minute period.
3. Geometric Linearity:	>3%	Max. deviation from a straight line of lines from a square grid scanned by the dissector.
4. Uniformity of Photocathode Sensitivity:	> ± 12%	Based on scanning a uniformly illuminated field; lens effects included.
5. Scanning Speed:	60 steps/second	Limited by incremental tape recorder. Tube and drivers are capable of operating at TV scan rates.
6. Required flux on photocathode:	.02 lumens	For 1.0μA photocathode current.
	>means "better than" here.	

The choice of scanning speed depends on the minimum allowable signal to noise ratio and on the writing rate of the recording instrument. S/N does fall off as scan rate increases hence it would not be possible to take 0.30% accuracy data at TV rates. Since the computed theoretical S/N at the 60 steps/sec. rate is 800, one can realistically expect to obtain S/N in the 300 to 800 range for the F4052 dissector at this scan rate.

The illumination requirement for the F4052 for the cited photocathode current of 1.0 microampere (S/N $\geq$ 300) is about 2 x 10^{-2} lumens on the photocathode. This may be satisfied with a 1 foot diameter integrating sphere illuminated by a 30 watt incandescent lamp for uniform illumination of a film transparency, or by a real illuminated scene having an average luminance of 15 ℓm/Sr. ft.^{2} ($\approx$50 ft.-L).

Two units, the camera, and the electronics rack comprise the Image Dissector Scanner. The objective lens, an optical focusing control, and controls for setting the dissector tube's voltages are mounted on the camera unit. A photocathode current meter and a photocathode voltmeter are also on the camera. The voltage controls are 10 turn clock dial types which permit easy resetting and recording of operational parameters. An automatic photocathode protection circuit (with indicator) and an anode pre-amplifier are also contained within the camera unit.

The electronics rack assembly is a floor unit about 6 feet tall and houses all necessary power supplies, logic cards, deflection yoke drivers, and display equipment for the scanner. A multi-conductor cable connects the rack to the camera thereby allowing positional flexibility between the two units.

After a warm up time of 1/2 hour, the scanner's output can be recorded with the accuracy and stability previously quoted. Internal logic allows operating the scanner in a sawtooth raster mode at a 30 Hz frame rate for setup purposes. Horizontal and vertical position controls allows freedom of movement of the scanning aperture position relative to the scene imaged on the photocathode. A CRT monitor mounted in the rack displays the scene under scan as adjustments are made. After setup the raster logic is disabled and the yoke drivers are switched to the externally supplied data scan signals for data acquisition. Any type of scan as desired can be used to drive the scanner.

4.3.3 Image Restoration Work Performed

In January of 1968 a study comparing the performance of the Image Dissector Scanner to that of Object Plane Scanner was completed. Transparencies of a turbulence distorted five and a quasi-point source distorted by the same turbulence were scanned by both scanners over an array of 64 x 64 picture elements. Both sets of scan data were then computer processed via image restoration techniques using the "point source" data plus "square frequency cutoff" filtering. Because of the inherent variability of the image dissector photocathode sensitivity a free frame or uniform field scan was made just prior to the image scans. The free frame scan data were used to correct the image scans so as to remove the effects of photocathode variability. After processing it was determined that all of the restored images were of comparable quality. Differences in the processed spectra prior to the final restoration are attributable to the difference in noise properties of the two systems and to the effects of the "square cutoff" filtering used on the two data sets.

4.3.4 Future Plans

The Image Dissector Scanner is scheduled to be moved to the IBM 1800 computer area where it can more easily be used for scanning tasks. Closer proximity to the computer facilitates interfacing with computer generated scan drive signals. Real time storage of the Scanner output in computer core would also be simpler to realize in the new location. This mode of operation would eliminate the need for recording data on magnetic tape, a time saving feature for certain exploratory studies where one might wish to quickly choose which of several possible viewing angles to use to acquire data for processing. This assumes viewing a real scene or a model of a real scene, a capability for which the Image Dissector Scanner is well suited. The sawtooth scan mode would be used to quickly view the scene at various perspectives and exploratory data scans could be taken and processed as a preliminary to fixing the desired setting. Use of the scanner in this mode eliminates the photographic and photo-processing procedures usually used to record a scene. This of course would save time and should also provide a more accurate measurement of the scene of interest.

A second generation packaging of the Image Dissector Scanner could be done which would produce a much smaller unit - one that would be more truly portable. The camera unit can be reduced to one-third of its present volume and the rack unit volume could be halved. While the present camera unit is portable it is sufficiently bulky to make it difficult to position in an elevated position or inclined at some elevation angle greater than 10 or 15 degrees. The present mechanical focusing lock is also insufficient for operation at medium or higher elevation angles. It thus is apparent

that to plan in terms of real scene viewing, real time operation, and re-packaging for improved portability is to plan to fully utilize the potential inherent in the Image Dissector Scanner.

4.4 Punched Card Recorder

The Punched Card Recorder, shown in Fig. 15, replaces the original scanner control electronics reported previously.[9] This system operates with any of the optical-mechanical scanning heads, digitizing the film transmission value and recording the number on punched cards via an IBM 526 summary punch. The system can also be operated in a playback mode and a polaroid print produced from a card deck.

The analog to digital conversion scheme employed consists of a Dymec voltage to frequency converter followed by a CMC counter. The counter gate is set at .1 seconds. An inherent advantage in this system is that it acts like a perfect integrator over this time interval. Hence there is no difficulty in achieving the required conversion accuracy of .01%.

After the data point value is digitized by the counter, it is transferred to a buffer storage and scanned by the 526 punch. The punch is allowed to run in the high speed duplicate mode (16-18 card columns/sec) and essentially clock the system. The punch is stopped at the end of each line to allow the stepping motors to retrace.

In the high accuracy mode, four digits and a space are allowed for each data point so that digitization proceeds at about 5/18 seconds per data point.

Playback is accomplished by switching the punch into read and transferring the data to a register in the logic unit. Here the data is operated

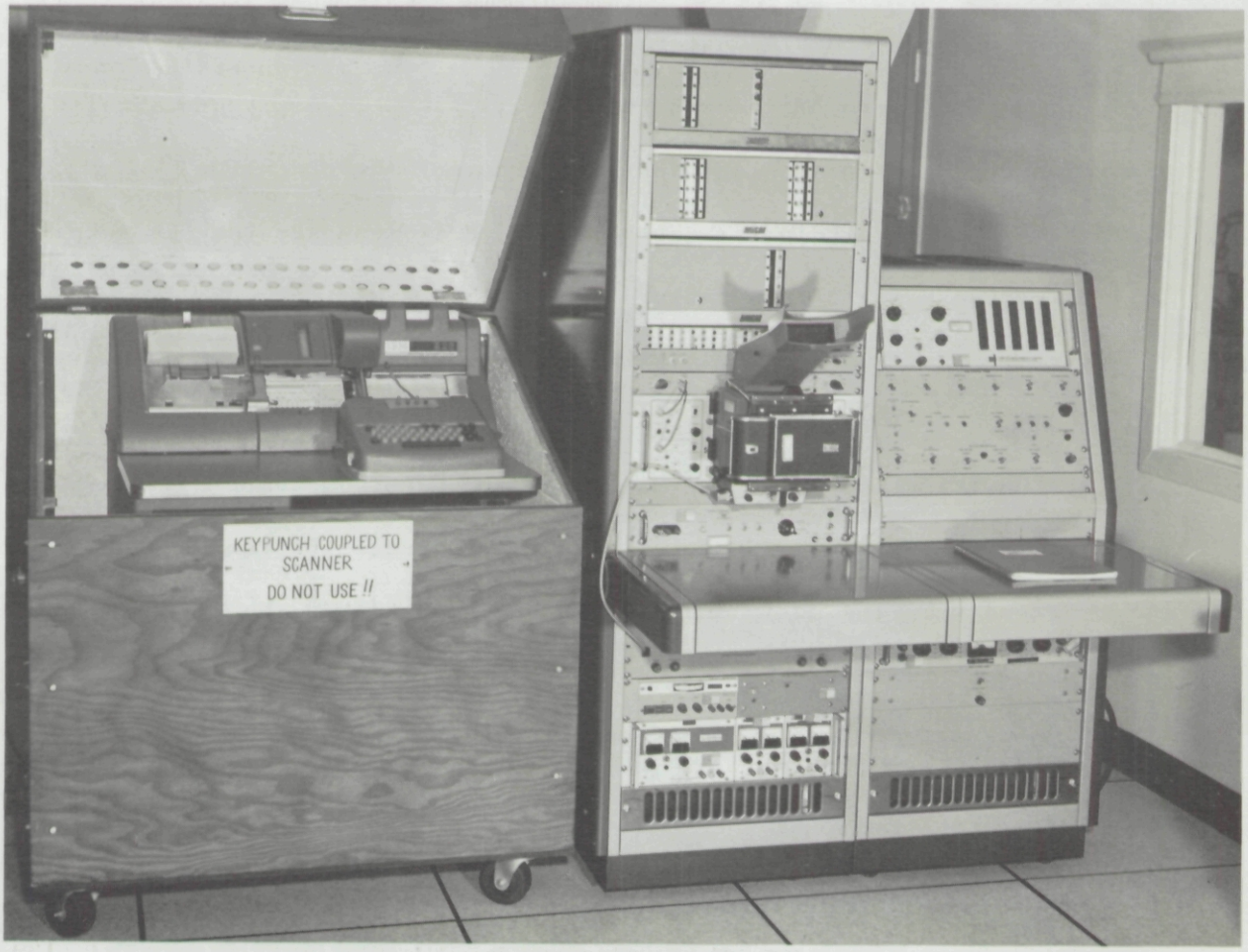

Fig. 15. The second generation Punched Card Recorder System.

upon by an digital to analog converter and a voltage to frequency converter. The latter serves as a gating source for the oscilloscope. A raster is generated by x and y counters which are preset by the operator. These are connected to D/A converters which drive the horizontal and vertical deflection amplifiers of the recording oscilloscope. A picture is also generated during recording and serves to monitor the operation.

A fewer number of digits, can be recorded if less accuracy is required. This of course results in a faster digitization time.

Any size raster up to 1024 x 1024 can be employed during record or playback.

This unit together with the Magnetic Tape Recorder comprise the two principal digitization equipments currently in use. The Punched Card Recorder results in the most accurate scan because it has the capability to integrate the MPT signal for .1 seconds. However, it is slower because of this. Card output is often more convenient than tape for handling and editing reasons. The Magnetic Tape Recorder, to be described in the next section, is faster with a corresponding reduction in accuracy.

4.5 Magnetic Tape Recorder

The Magnetic Tape Recorder, shown in Fig. 16, is an electronic console that can utilize any of the optical-mechanical scan heads as an input. It will digitize the data as a four bit BCD encoded number and record it on seven level magnetic tape at a 300 character per second rate. Data encoded in a similar format can be read from tape at the same speed and a photograph generated. By means of a keyboard the operator can write identification data on the tape. A twelve digit word setup by thumbwheel switches can be recorded by pushing a button.

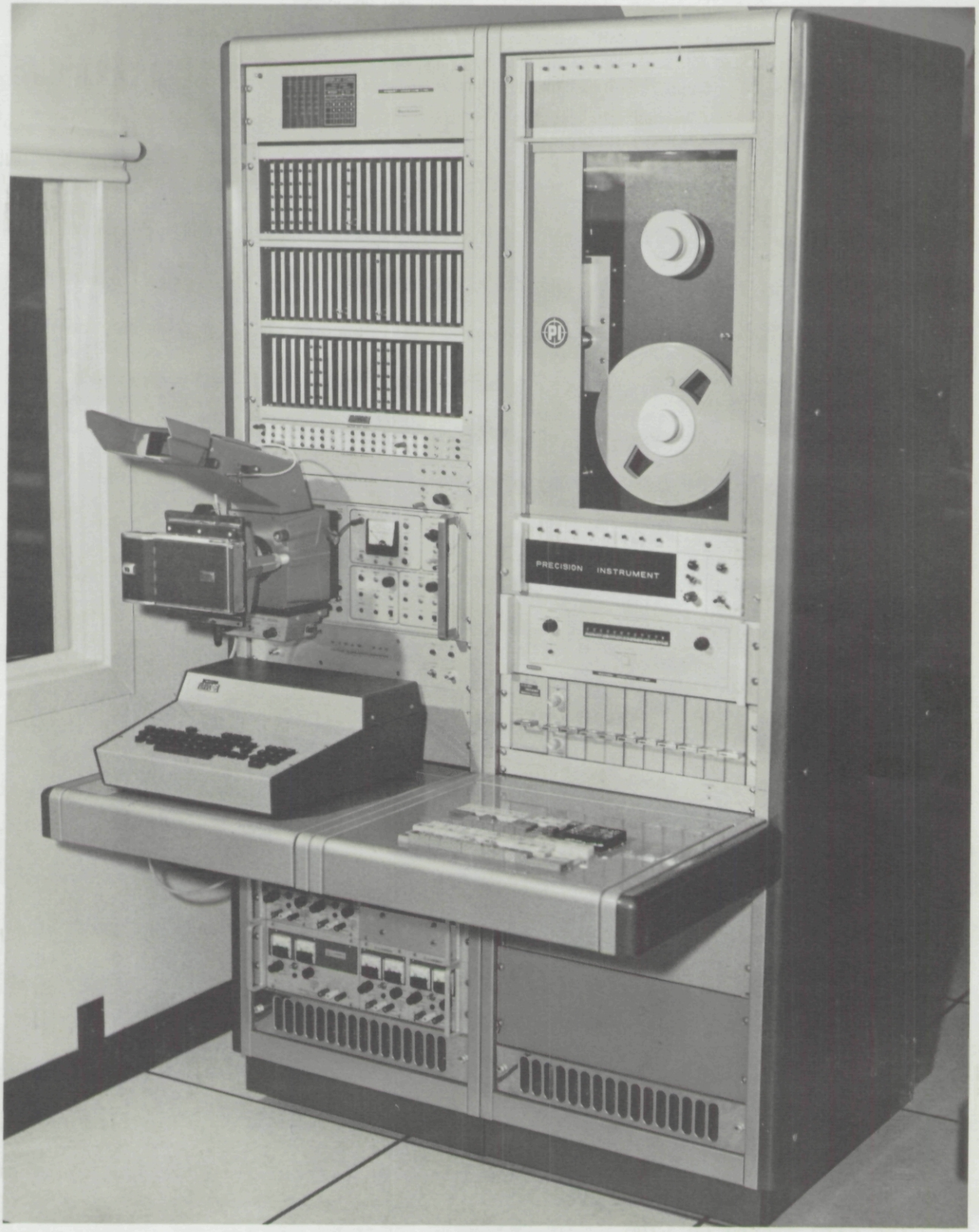

Fig. 16. The Magnetic Tape Recorder System.

Certain tape search operations are also possible. The machine can be operated in slew speed (600 characters per second) and a search made for file marks or certain identifying characters, permitting the operator to search for a given record.

When used in the recorder mode the scanner phototube signal is amplified by a Beckman variable Bandpass "amplexer" amplifier. At this point the pass band can be matched to the data rate. Digitization is performed by a Beckman 4040 A/D converter and converted from parallel to serial form by a Beckman 3104 Intercoupler. The recorder employed is Precision Instruments 1107 incremental recorder. Each data point is recorded as four BCD characters followed by a space character. If less accuracy is required a fewer number of digits may be recorded.

A Navigation Computer Corporation keyboard has been interfaced to the system enabling the operator to record alphanumeric information on the tape at the beginning of a scan record. A fixed identification number, setup by thumbwheel switches, can also be recorded on the tape by pushing a button. Each of these special identification records as well as the data record is identified by a special character and separated by an end of record gap.

When used in the picture playback mode data is incrementally read from the tape one character at a time at a 300 character per second rate. The set of characters comprising one data value is stored in a register and then converted into frequency by a D/A converter and a Vidar 240 voltage to frequency converter. The resultant frequency time gates a modified HP 140A oscilloscope. A time exposure photograph of the CRT produces a picture of the data stored on tape.

Any raster size up to 1024 x 1024 can be accommodated. The size of the raster is programmed into the system by the operator.

The tape can be read in slew speed (600 characters per second) and searched for end of file marks, end of record marks or certain numbers in the fixed ID records. Thus a particular record can be sought out and a picture made of this record. An alternate option is to search through a given number of EOF marks.

Certain test or experimental features have been incorporated. The following is a list of a few of these:

a.) Stepping motors off

b.) Incremental stepping by means of a push button

c.) Data point by data point stepping by means of a push button

d.) External clock

e.) Z axis non gated

f.) EOF disable

4.6 Remote Scanning Console

The Remote Scanning Console, shown in Fig. 17, is used to accurately position the start of a scan before the actual scan is undertaken. By means of push buttons, the operator has direct control over the stepping motors and can advance or reverse them either one step at a time or at a slew rate. Counters on the unit record the number of steps taken.

Some of the operations that can be performed are fairly sophisticated. As an example, the operator can position the stepping motors to a given position and reset the counters. The counters can now be preset in X and Y and the stepping motors will advance to the preset point. Thus one can accurately and repeatedly advance to any point on the film from any starting point and return to the starting point.

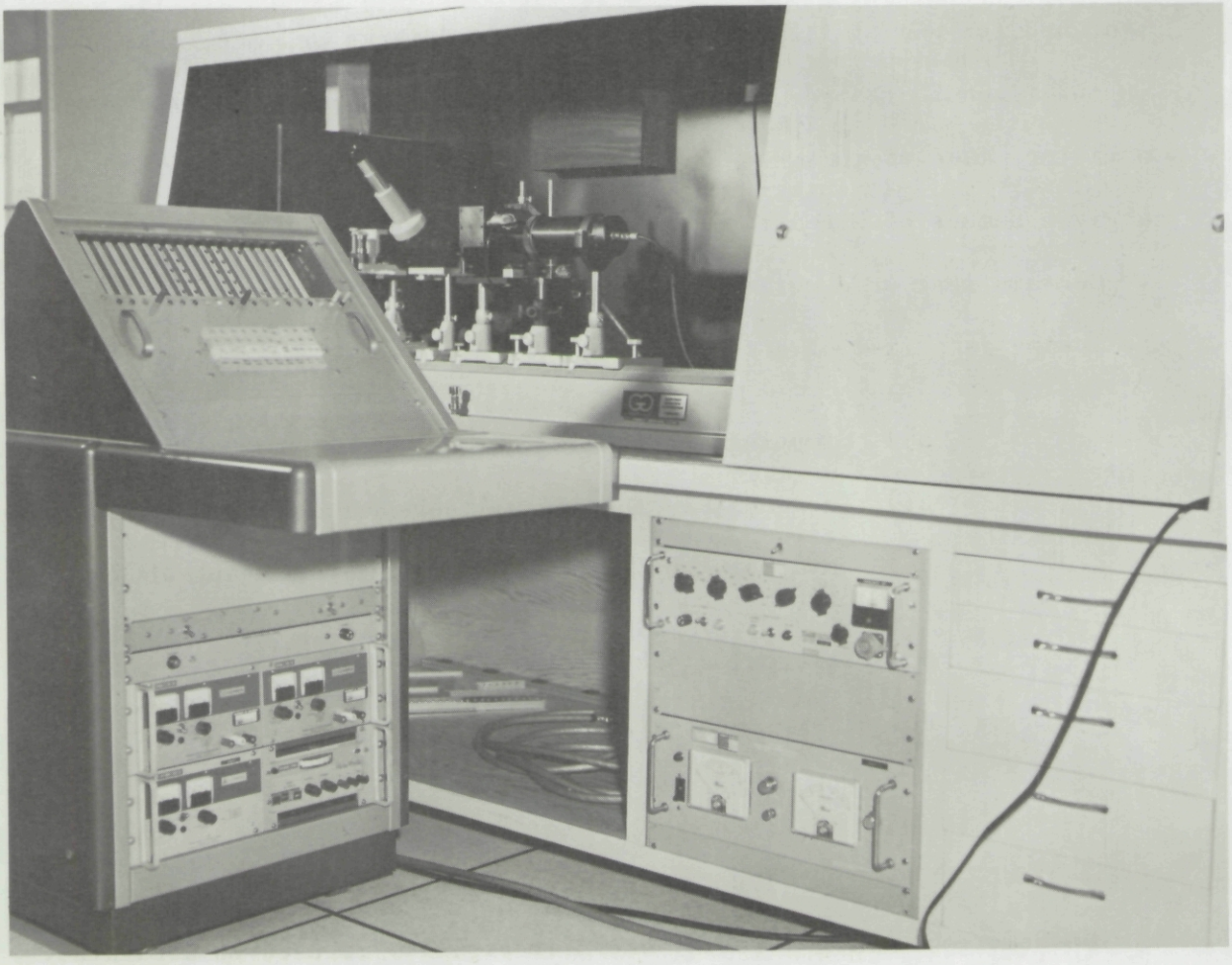

Fig. 17. The Remote Scanning Console.

4.7 1800 Refresh Display*

At the present time the 1800 Refresh Display is being integrated into the image processing system. It will take over all of the display and picture generation functions currently being performed. The system that is currently handling these tasks is an interim system that produces graphics on a Tektronix 564 storage scope and polaroid pictures on a Tektronix 503 oscilloscope. These units are connected to X, Y and Z axis D/A converters in the 1800 computer. The Z axis modulation for the polaroid pictures is produced by a time gate derived from a Vidar voltage to frequency converter that is connected to the Z axis D/A converters. Synchronization and gating is accomplished by means of the 1800 digital output register. Since this interim system is currently being replaced it will not be described in any further detail.

4.7.1 General Description

The Refresh Display System is shown in Fig. 18. The system receives digital instructions and data from the 1800 computer. The data is stored in a 4096 x 8 bit core storage. The instructions are eight bits in length and executed as they are received. In this mode the system is entirely under 1800 control. Upon command it will receive a matrix and present it as an intensity modulated display that recycles at a 50 Hz rate. It can also produce a 3-1/4 x 4-1/4 polaroid print or a 16mm frame. A choice may be made between the conventional square spot or the inner raster picture generation techniques (see Sec. 4.7.4).

Graphical information from the 1800 is transmitted to the system in analog fashion. It is presented to the user in the form of a stored display. This data can also be automatically photographed on polaroid or 16mm film.

*This system was developed under other funding.

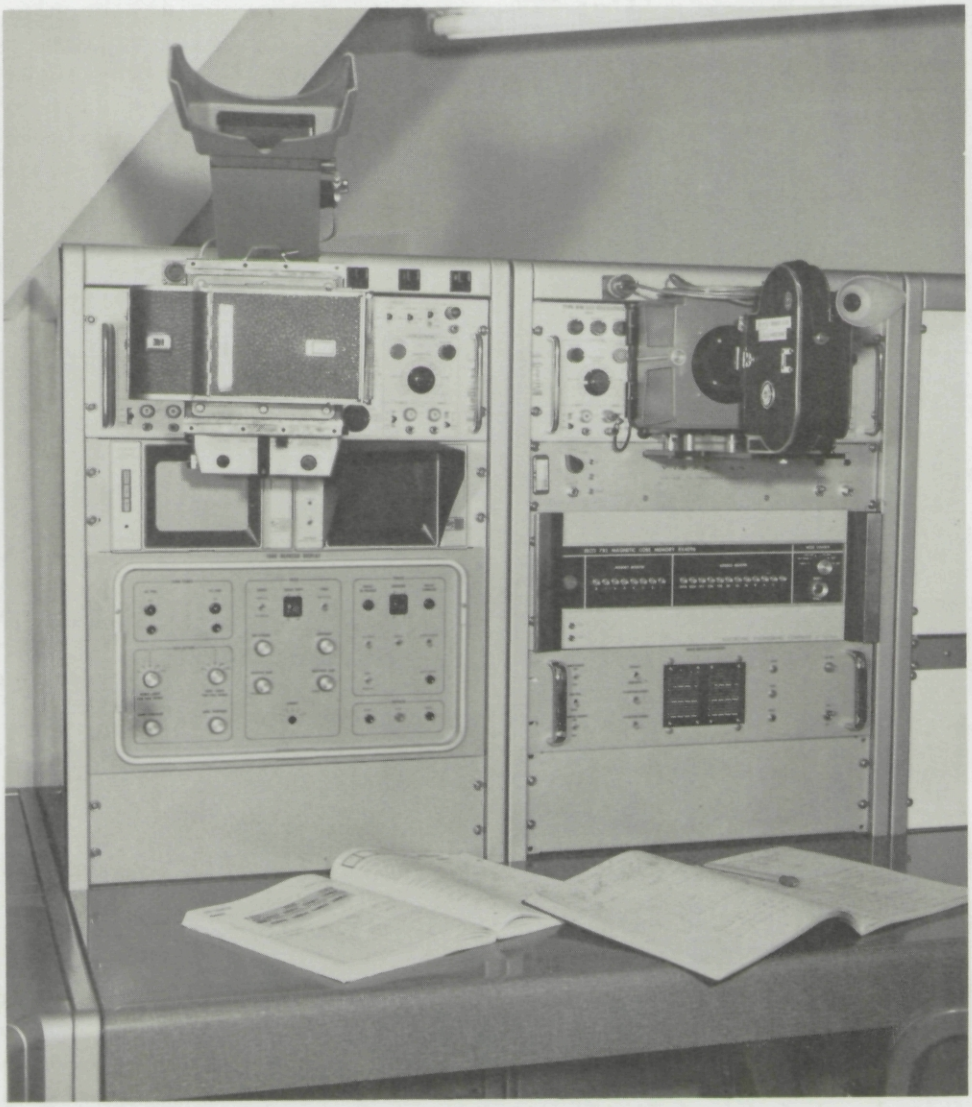

Fig. 18. The Refresh Display System.

After a picture matrix has been transmitted to the system, the computer is free to continue with other processing. At this point the user is free to assume control and manipulate the data further, observing the result on the refresh display. At any point the user may elect to make hard copy prints of the results.

The various operations that can be performed on the data fall into the two catagories of analog and digital. The user can invert or rectify the data digitally or a shifting operation can be performed. The analog controls available are brightness, contrast, positive/negative clipping and gamma.

When a picture is generated by the square spot method, only the effects of the digital processing controls are present. The reason for this is that the modulation for this technique is a variable stepping rate derived from counting down the digital intensity values. When the inner raster is employed a digital to analog conversion is employed, hence, the user can elect to have the photograph mirror the effect of the analog controls if desired.

4.7.2 Instruction set

The instructions to the system from the computer are eight bit words. The first four bits are refresh display instructions, the last four bits being camera instructions. The refresh display instructions are:

1. Load X
2. Load Y
3. Load Z
4. Unload Z
5. Reset Core Z
6. Master Reset (excluding core Z)
7. Refresh Start
8. Refresh Stop
9. Video switch to include analog controls

The camera instructions are:

Bit 1 - Graphics

Bit 2 - Polaroid Camera

Bit 3 - Bolex 16mm Camera

Bit 4 - Inner Raster on (If this bit is zero, the square spot method is in effect)

4.7.3 Refresh Display and Video Processing

The display employed is a Tektronix 602 oscilloscope with a P4 phosphor. The data rate is 200k Hz; so that a 4096 array repeats at about a 50 Hz rate. The intensity values are stored as 8 bit binary numbers, the most significant bit representing the polarity bit. Normally the 1800 scales the values to the range of -127 to +127. Thus the intensity resolution of the system is one part in 256.

The following processing options are available:

1. Video shift - The digital representation of the intensity value can be shifted to the right 1, 2, or 3 places. The result of this is to emphasize low order background variations.

2. Invert - This is a digital operation in which the polarity bit is inverted and the complement is taken.

3. Rectify - This also is digital. In this case the polarity bit is ignored and treated as positive.

4. Brightness - A shift in the DC level of the video.

5. Contrast - A variation in the amplitude of the video signal.

6. Positive Clip - The black level of the video remains fixed and the highlights are clipped.

7. Negative Clip - The highlight level of the video remains fixed and dark level is clipped.

8. Gamma - An analog operation in which the amplitude of the video is raised to a power. The exponents that may be selected are .25, .5, 1, 1.5 and 2.

4.7.4 Picture Generation

In the playback of a discretely sampled image some method of interpolation between adjacent sample points is necessary to avoid distracting effects on the human visual system. The refresh display system employs two methods to accomplish this. In the square spot method a high speed 16 element matrix is generated to create a series of tangential squares. Modulation with the intensity values is accomplished by transferring the digital value into a register and counting it down to zero, causing the square to remain stationary for this length of time. The result is a variable stepping rate that is inversely proportional to the intensity value. The count down clock can be varied over a ten to one range by means of a front panel, thumbwheel control. For a full scale brightness value of 256 the shortest count down time is about one millisecond. Thus a matrix composed of 4096 values of 256 would generate a picture in about 4 seconds. The average picture however would be generated in less time since some low values of brightness would be encountered.

In the inner raster method an inner raster generator produces a sequence of overlapping squares, each square being twice the size of a matrix element. The square is made up of a sequence of 256 discreet spot positions. The intensity of the spot varies in both X and Y in accordance with the product of two functions of X and Y respectively. These functions are programmable from the front panel. In this fashion a spatial filtering is achieved. Usually the functions are chosen so that no background modulation is present. The matrix information modulates the scan by means of an on-off blanking technique. A Vidar voltage/frequency converter is modulated with the video signal to produce this blanking pulse. The video signal can be obtained before or after the video processing section at the discretion of the operator.

Two Tektronix 503 oscilloscopes receive the picture raster in parallel. A polaroid camera is connected to one and a bolex camera to the other. Either or both shutters can be activated by the operator or the computer, as the system sweeps out the picture.

4.7.5 Graphics:

In this operation the X and Y digital to analog converters (DAC's) of the IBM 1800 are connected to a Tektronix 601 storage scope. Upon receipt of a graphics command, the 1800 Refresh Display System also switches the 1800 DAC's to the camera scopes in lieu of the normal connection to the internal system DAC's. Thus, if desired, the graphical information may be photographed.

4.8 Research Equipment

An experimental equipment complex has been developed to aid in the design of digital processing equipment. Included here are a flying spot scanner, a magnetic tape recorder a refresh display system, and a polaroid print generation system.

4.8.1 Flying Spot Scanner and Recorder

The magnetic tape recorder is a Precision Instrument, Model 1207. It has been interfaced to read or write at high speed (37 1/2 ips) or slow speed (4 ips write, 1.6 ips read). When writing, the recorder is connected to the flying spot scanner. The material to be scanned is mounted in a 35mm transparency mounting and inserted into the scanner. The material can be converted into a matrix of any size up to 1024 x 1024. The transmission values of the film are converted into 3 BCD digits. Each digit occupies one frame of a seven level tape. The data values are separated on the tape by a space character. One, two, or three digits may be recorded at the discretion of the operator. Standard end of file and end of record gaps are inserted.

A tape may be read at high speed or slow speed and the information transferred into the core storage. Alternately a picture may be generated directly as the tape is read. The format of the tape can be flexible in that there may be one through seven characters per word.

4.8.2 Core Memory and Refresh Display System

The core memory previously used in this system was a 4096 x 8 bit, 5μ-sec. cycle time unit manufactured by Engineered Electronics Company. This unit was transferred over to the 1800 Refresh Display System. The unit currently being interfaced in its place has a capacity of 4096 x 24 bit and a cycle time of 1.6 μ-sec.. It is manufactured by Varian Data Machines.

The system will be described as it operated with the EECo core since the Varian core has yet to be integrated into the system.

Data was stored as two BCD digits per data point. Thus a 100:1 range in intensity was possible. When converted to the refresh display, data was unloaded at a 125k Hz rate. This was done in an interlaced, line-locked fashion. Each field would unload in 1/60 seconds, the frame rate being 30 Hz. The controls available to the operator were video gain brightness and focus.

4.8.3 Camera Unit

To produce a photograph a time gate is produced whose duration is proportional to the length of time necessary to count the z axis register down to zero. The clock rate employed is 300k Hz.. At this rate, only 1/3 milliseconds is needed to count down the largest z axis value. Because of this a picture can be made at high speed (37 1/2 ips) from the tape providing at least two digits and a space are recorded per data point.

A picture can also be made from the core by having it serve as the input to the count down circuit.

The flying spot scanner referred to is a dual channel phototube system designed and constructed at the Visibility Laboratory. It utilizes the same optics and mounting as a Tektronix C-12 camera system. One channel can serve as a monitor although this feature has yet to be used. The optical unit can be mounted on any oscilloscope to which a C-12 mounting adapter can be attached. Oscilloscopes that have been used with the system are the Tektronix 503 and Celco High Resolution CRT unit with magnetic deflection.

5.0 SUMMARY

The status and direction of the major areas of our research will be briefly summarized.

Processing methods for restoration of images which are limited by noise have concentrated on Fourier techniques. Present emphasis is on methods to approach the effectiveness of the least squares filter (The least squares filter itself cannot be used since it requires information not usually available). Significant improvements beyond this level will probably involve completely new approaches governed by statistical decision theory. Research will be directed into this area.

The restoration of images for which the point spread function is not initially known continues to be an important problem. Initial experiments in this area, which will be reported later, have been very encouraging. This is part of a broader area of methods of utilizing a priori knowledge in the restoration process. Work will also be directed in this area.

The limited number of sensor studies made have demonstrated the need for more extensive data on film characteristics. Comparative tests have indicated that among films 3404 is the most effective of those tested. The tests also indicate that the image intensifier is potentially a good sensor for image processing applications.

The computer facility has proved to be a very important part of the research effort. The modular approach to image processing operations on the computer has been found to be extremely useful both in on-line operations and production type runs. A particular capability which should find more use in the analysis of optical systems is the ability for optical system simulation. There are several areas which need improvement in the computer facility. For some operations, particularly those in which modification of selected parts of a matrix is desired, communication with the computer is still slow. New devices, such as a light pen system and thumbwheel entries, will be developed which will allow more rapid communication between the experimenter and the computer. The ability to process arrays larger than 64 x 64 is needed and will be developed during future work.

Equipment development has, as in the past, played an important part in the research. The present equipment facility has been adequate for most image processing needs. Future work will concentrate on development of the light pen system and other devices to aid in on-line processing.

ACKNOWLEDGEMENTS

This report was written by several staff members of the Visibility Laboratory. Each wrote on the portion of the research for which he had the major responsibility. The authors of the various sections were:

Section 1 and 2, B. L. McGlamery;

Section 3, Madison L. Myers;

Section 4 (exclusive of 4.2 and 4.3), Richard L. Ensminger;

Section 4.2, B. L. McGlamery;

Section 4.3, Robert F. Howarth.

UNCLASSIFIED
Security Classification

DOCUMENT CONTROL DATA - R&D

(Security classification of title, body of abstract and indexing annotation must be entered when the overall report is classified)

1. ORIGINATING ACTIVITY *(Corporate author)*
Visibility Laboratory
University of California
San Diego, California 92152

2a. REPORT SECURITY CLASSIFICATION
UNCLASSIFIED

2b. GROUP

3. REPORT TITLE

PROGRESS IN IMAGE PROCESSING TECHNIQUES AND EQUIPMENT

4. DESCRIPTIVE NOTES *(Type of report and inclusive dates)*
Final Report

5. AUTHOR(S) *(Last name, first name, initial)*

McGlamery, Benjamin L., Myers, Madison L., Ensminger, Richard L., Howarth, Robert F.

6. REPORT DATE	7a. TOTAL NO. OF PAGES	7b. NO. OF REFS
November 1969	81	10

8a. CONTRACT OR GRANT NO.	9a. ORIGINATOR'S REPORT NUMBER(S)
F08606-68-C-0017 Mod P003	SIO Ref. 69-28
b. ARPA Order No. 1062, Amendment No. 1	
c.	9b. OTHER REPORT NO(S) *(Any other numbers that may be assigned this report)*
d.	

10. AVAILABILITY/LIMITATION NOTICES

Distribution of this document is unlimited.

11. SUPPLEMENTARY NOTES	12. SPONSORING MILITARY ACTIVITY
	Advanced Research Projects Agency Washington, D. C. 20301

13. ABSTRACT

This report describes the current emphasis of image processing research at the Visibility Laboratory. The following aspects of the work are described: image processing studies, sensor studies, the image processing computer system and image processing equipment. The image processing studies compare the performance of different methods of image restoration as a function of noise level in the degraded image. The sensor studies compare the noise characteristics for several different sensors used for recording images. The capabilities of the computer system used for image processing and the program philosophy are described. The characteristics of the image scanning and display systems used as input and output devices for the image processing facility are reported.

DD FORM 1 JAN 64 1473

UNCLASSIFIED
Security Classification

14 KEY WORDS	LINK A		LINK B		LINK C	
	ROLE	WT	ROLE		ROLE	WT
Image processing						
Image restoration						
Image evaluation						
Computer image processing						